NTNU
Norwegian University of
Science and Technology

Analysis of accidental iceberg impacts with large passenger vessels

Suyu Wang

Marine Technology
Submission date: June 2017
Supervisor: Jørgen Amdahl, IMT
Co-supervisor: Ekaterina Kim, IMT
Zhaolong Yu, IMT

Norwegian University of Science and Technology
Department of Marine Technology

NTNU
Norges teknisk-naturvitenskapelige universitet
Institutt for marin teknikk

MASTER THESIS 2017
for
Stud. Techn. **Suyu Wang**

Analysis of accidental iceberg impacts with large passenger vessels
Analyse av ulykkesstøt fra små isfjell mot passasjerskip

The sea ice extent and thickness in the Arctic have diminished over the past few years due to global warming. This diminishing ice may provide access to new sailing routes in these waters in the years to come. Thus Arctic waters are becoming attractive due to the large reservoir of oil and gas, ship transport in the NE or NW passage as well as touristic attractions. Activities in such areas will, however, meet with harsh environmental elements, such as ice loads and low temperatures. Darkness and remoteness from infrastructure and search and rescue services increase the potential consequences of accidents with respect to loss of lives, property damage and environmental pollution. The probability of collisions between ships and icebergs may increase due to this increased activity. The assessment of the loads caused by iceberg impacts is an important issue for ship designers. In modern ship and offshore structure design, the design should always be carried out under the principle of the Ultimate Limit State (ULS) and further checked with the requirements for the Accidental Limit State (ALS).

Although it is not explicitly stated, the conventional design of ship structures is carried out in the ULS format. This design implies that the structure is only allowed to undergo small deformations with no or limited elasto-plastic behaviour. The task is then to determine the scantlings such that the structure can resist the maximum pressures and forces from the ice as the ship is crushing the ice. Consequently, the ice action is often characterised as pressure versus contact area curves; the smaller the contact area, the larger is the indentation pressure. Substantial efforts have been invested over the past decades to determine pressure-area relationships for crushing ice. A variety of formulations can be found in ship classification codes and rules for arctic offshore structures, such as IACS and ISO 19906. The return periods for the ice pressures are not always explicitly stated, but in general, vary from a few years to 100 years.

Pressure-area relationships are sometimes also given for very rare ice impact events, for example, for a return period of 10000 years. The intention is to use the pressure for design in the ALS format. Such pressure–area relationships are useful if the objective is to design the structure to be so strong that it can crush the ice with very moderate deformations, similar to the task in the ULS design. This approach will often lead to overly conservative design. In most codes, it is accepted that the structure may undergo substantial deformations in the ALS design; yielding, plastic mechanisms, buckling etc. are allowed, but the integrity of the structure with respect to global stability shall not be put in jeopardy. For a ship or offshore structures carrying dangerous cargo, it is also normally required that a spill into the environment should not occur. For a double-hull tanker, this requirement implies that, while gross deformation and fracture of the outer shell may be accepted, puncturing of the inner shell (cargo tank) should not occur. For this kind of design, pressure-area curves are meaningless; the structural resistance will to a large extent limit the pressures on the ice-structure interface.

Icebergs may take on a variety of shapes. A few attempts have been made to characterise the shapes, but so far, a common agreement on standard shapes to be used for ALS design has not been established. An alternative approach to characterisation of iceberg shapes on the basis of empirical surveys is to characterise the shapes in view of *the structural resistance* to iceberg impacts. In principle, a "spear-like" protrusion of an iceberg has a large puncturing potential, but in such cases the side of the ship will simply crush the ice. A vertical, plane iceberg surface yields significant confinement of the ice, which may become virtually rigid compared to the structure. However, the associated large contact area yields a significant energy dissipation capability, and no penetration of the inner hull is likely (unless the iceberg kinetic energy is very large).

The objective of the present work is to assess the resistance of a large, moderately ice-strengthened passenger vessel to ice floe/bergy bits ice impacts.

The work is proposed to be carried out in the following steps:

1. A brief discussion of potential impact scenarios and how this may be modelled for nonlinerar finite element analysis.

2. Establish a finite element model of the side structure in the bow shoulder area for a large passenger vessel for analysis with LS-DYNA. The size of the modelled area is to be decided in collaboration with supervisors. The model should extend beyond the ice strengthened region to allow simulation of impacts for sea-going vessels. The choice of the model, boundary conditions etc. shall be thoroughly discussed. Material rupture shall be represented with the RTCL or extended BWH model.

3. Establish a finite element model for the ice floe/bergy-bit ice for a few selected shapes. The shapes should be selected with due considerations of the side geometry. Select ice material parameters such that desired pressure-are relationships are regenerated for ice crushing against a rigid wall.

4. Perform integrated simulations of impact from the selected iceberg shapes and contact locations. The simulations should preferably include cases with rupture of the outer shell. The results form the simulations shall be thoroughly described and discussed with respect to failure modes of plating, stiffeners, frames etc. and the share of energy dissipation in the shipside. Document interface pressures and discuss their magnitude in view of the ice material model.

5. By means of external mechanics considerations, determine the critical relative speed for penetration of the outer shell.

6. Conclusions and recommendations for further work

Literature studies of specific topics relevant to the thesis work may be included.

The work scope may prove to be larger than initially anticipated. Subject to approval from the supervisors, topics may be deleted from the list above or reduced in extent.

In the thesis the candidate shall present his personal contribution to the resolution of problems within the scope of the thesis work.

Theories and conclusions should be based on mathematical derivations and/or logic reasoning identifying the various steps in the deduction.

The candidate should utilise the existing possibilities for obtaining relevant literature.

Thesis format

The thesis should be organised in a rational manner to give a clear exposition of results, assessments, and conclusions. The text should be brief and to the point, with a clear language. Telegraphic language should be avoided.

The thesis shall contain the following elements: A text defining the scope, preface, list of contents, summary, main body of thesis, conclusions with recommendations for further work, list of symbols and acronyms, references and (optional) appendices. All figures, tables and equations shall be numerated.

The supervisors may require that the candidate, in an early stage of the work, present a written plan for the completion of the work. The plan should include a budget for the use of computer and laboratory resources, which will be charged to the department. Overruns shall be reported to the supervisors.

The original contribution of the candidate and material taken from other sources shall be clearly defined. Work from other sources shall be properly referenced using an acknowledged referencing system.

The report shall be submitted in two copies:
- Signed by the candidate
- The text defining the scope included
- In bound volume(s)
- Drawings and/or computer prints that cannot be bound should be organised in a separate folder.

Ownership
NTNU has according to the present rules the ownership of the thesis. Any use of the thesis has to be approved by NTNU (or external partner when this applies). The department has the right to use the thesis as if a NTNU employee carried out the work, if nothing else has been agreed in advance.

Thesis supervisors
Prof. Jørgen Amdahl

Co-supervisors
Post.doc Ekaterina Kim, Zhaolong Yu

Deadline: June 10, 2017

Trondheim, January 11, 2017

Jørgen Amdahl

Summary

The number of collisions between ships and ice are increasing with the increase of ships sailing in Arctic areas. It is necessary to research on large passenger ships subjected to iceberg impact, since it may cause huge human life loss.

The method to design ice going ship nowadays is presented. The conventional design of ship structures is carried out in the ULS format. But the design of ship-iceberg impact scenario should fall into ALS design, due to its rare and large load property. ULS design for ship-iceberg collision will yield over-designed structures. The method to get the design ice load according to IACS Polar Class rules is introduced. The design method is based on simplified method and it doesn't take the ship-iceberg collision into consideration.

For engineering calculations it is common to decouple the collision event into external and internal mechanics. The basic ideas about splitting the impact process into these two parts is introduced. Some numerical simulation cases in Liu's paper are also presented to give a more clear introduction. The internal mechanics depends on the relative strength of the ship structures and Iceberg, so it is necessary to establish an accurate ice material model. The most important mechanical and physical properties of ice are described. The material model for iceberg developed by Liu is also presented. The numerical simulation using this ice material is also presented to show that this ice material model is validated.

The major work in this master thesis is to establish an FE model for both ship structures and ice floe, and then run impact simulations in Ls-Dyna. The establishment of FE model of ship structures and Ice floe is introduced in detail. The impact analysis setup in Ls-Dyna prepost is also presented. Some key points about how to get appropriate numerical simulation results are presented for anyone who wants to do this kind of analysis again.

The simulation results are presented in detail. Basically, the ship is designed with enough resistance against ice floe impact load. The ship can crush the ice completely without being significant damaged. One simulation was run using rigid material, and the ship shell was easily penetrated. The damage pattern of the ship structures is analyzed for this simulation. Some simulations were run with an error, which makes the ice uncrushable. In these cases, the ice floe will cause significant

deformation on the ship shell but not penetrate it. The results are also presented to make a comparison with the crushed ice.

Preface

This report is the result of the Master Thesis work for student Suyu Wang, in Marine Department at the Norwegian University of Science and Technology, NTNU, spring 2017. The work has been carried out as a continuation of the Project work carried out in fall 2016. The main objective of this project is to analyze large passenger vessel subjected to Bergy-bit ice/ ice floe impact. From the project work, I have understand the background theory and the basic method to do this analysis. However, I still met quite many challenges during this thesis work.

The first challenge I met in this work was to establish a FE model for a ship structure. Before doing this thesis work, I have never established a FE model for a real ship structure. The geometry and scantling data were read from the ship drawings, so the first task is to understand the ship drawings. After looking over the drawings again and again and comparing the drawings from different perspectives, I have understand the construction of the structure in general and also found the specific scantlings for different parts. Then it was a challenge for me to model the ship surface, since the ship side is curved in 3D space and lack of ship cross-section drawings. That is solved by smoothing the ship line in AutoCAD. During the modelling work in the MSc. Paran, I really experienced great progress. During the process, I have always found more efficient and correct way to establish the model. Some tasks, which in the beginning could take hours to perform, could be solved in a few minutes at the end of the modelling process. Because of the geometry of the ship structure is quite complicated and irregular, I met great challenge while connecting some parts together, for example connecting the transverse frame on ship shell with deck. Besides, lots of efforts have been made on meshing the model without introducing very small and sharp elements.

The ice model is much simpler to establish compared to the ship structures. However, I met some challenges in the setup work for collision analysis. At the beginning, after contact, the ice slip down along the ship surface without causing considerable collision. Some different methods have been tried to prevent the ice from slipping down. Finally, it is solved by adding one extra boundary condition for the ice model. Besides, I have struggled dealing with negative sliding energy appeared in some simulation results, but after comparing and analyzing all the simulations I have made, the consequence of it is still not found at the end. To find the consequence, more simulations with different input is required, but there is no time left for doing this.

Unfortunately, an error has been made in the ice material model, which hasn't been found until when it came to the end of the thesis work. That mistake made the ice model uncrushable, so the ice appears too ductile. That mistake was corrected and several simulations with the correct input were run. But there is no time left for more simulations. One challenge in this master thesis work was the computing resources. For some reasons, I can only run the simulation on my personal computer, so the computing time is very long. For one simulation, it takes average 9 hours using 4 CPUs.

I would like to thank my Master Thesis supervisor Professor Jørgen Amdahl ,Ekaterina Kim and Yuzhao Long for good discussions and guidance during this thesis work. Without their guidance and motivating discussions, it had been really difficult for me to obtain satisfying results. I would also like to thank Ph.D. Yanyan Shan for helping me a lot during the modeling work and always being available for questions and giving me suggestions for solutions.

Tyholt, Trondheim, June 10,2017
Suyu Wang

Table of Contents

List of Figures

List of Tables

Chapter 1

Introduction

Due to the global warming, the sea ice extent and thickness in the Arctic area has diminished significantly over the past few years, which makes some new shipping routes possible. With these new shipping routes, the distance of traditional routes can be reduced by one-third. If these routes become reliable, the Arctic may become one of the world busiest shipping areas.

However, due to the harsh environment in Arctic area, ships operated in Arctic area have to be designed with more strict rules and special requirements than the sea-going ships. For example, Ships have to be designed with enough resistance to the ice load. The accidental collision between ships and bergy-bit ice and ice floe can happen and can cause huge human and property loss. One of the biggest disaster in marine history, Titanic, is the most obvious example. With the increasing of sailing routes in Arctic area, the probability of collisions between ships and ice may increase. The assessment of the loads caused by ship-ice impact is an important issue for ship designers to make sure that the ship maintains a sufficient safety level.

Because of the high-tech radar and satellite system, it is very rare to collide with a big or medium iceberg, like Titanic, nowadays . But it is still unavoidable to collide with small bergy-bit ice or ice floe which is quite difficult to detect before collision. This type of collision can also cause huge damage to ship structures.

For example, the Overseas Ohio directly hit an iceberg on the 2nd of Jan., 1994. The bulbous bow was ruptured and the ballast tank was holed. The cost to repair the damage is at least 1 million dollar.

Figure 1.1: Damaged bow of Overseas Ohio after collision with iceberg[6]

It is necessary to research on the effect toward ship structures, especially for passenger ships, from ship-ice collision, because these collisions may cause huge human loss. However, there is no previous analysis of large passenger ships subjected to accidental ice load having been done before.

The main part of work in this thesis is to study the behaviour and resistance of a large passenger ship subjected to accidental bergy-bit ice or ice floe impacts, by doing NLFEA simulations. A detailed Finite Element model of shoulder area of a passenger ship was made and analyzed for different impact scenarios. RTCL Material failure criterion was introduced to capture the likely fracture on the side shell. A continuum-mechanics model of ice developed by Zhenhui Liu was used to simulate the behaviour of ice.

Chapter 2

Review of ULS and ALS

In modern ship and offshore structure design, the design should always be carried out under the principle of the Ultimate Limit State and further verified with the requirements for the Accidental Limit State.

The ULS typically refers to design checks of components under functional and environmental actions with annual probabilities of occurrence in the range of 10^{-2}. The structure is only allowed to undergo small deformations with no or limited elasto-plastic behaviour. Thus the resistance is predominantly based on elastic resistance models. Yield stress is often set as the limit state.

The ALS check is a survival check of the structural system which is damaged due to accidental actions or environmental actions with annual probabilities of 10^{-4}. The structure may undergo yielding, buckling and large permanent deformations on its member and sub-structure levels, but the overall integrity will not be impaired. Thus, the resistance of the structure exceed the elastic domain, and is dominated by plastic behaviour. The resistance may be assessed by non-linear analysis methods.

In the ISO (2010), the ice actions associated with the ULS and ALS design checks were denoted as extreme level ice events (ELIE) and abnormal level ice events (ALIE).[8] ELIE implies that the structure is only allowed to undergo small deformations with no or limited elasto-plastic behaviour. The task is then to determine the scantlings such that the ship can resist the maximum pressures from the ice while crushing the ice for a given area depends on the layout of the shell plates. The design idea is that the ship is strong enough to simply crush the ice without excitation of large motion or large deformation. Then the contact force should be limited by the ice material resistance, so it maybe reasonable to think that the contact force is somewhat a material constant of ice. Consequently, the ice action is characterized as pressure versus contact area curves, the smaller the contact area, the larger the indentation pressure is.[8] As it is shown in the 'Ice Rules' part later, the assumed pressure-area relationship is one of the basic assumption to derive the design ice load in ice rules nowadays.

For a normal ice action, such as level-ice action, it is reasonable to use ELIE. However, for a ice actions with return period of 10000 years, if it is still only allowed to undergo small deformations like in ELIE, it will often lead to overly conservative design, which will then make the ship over safe but heavier and more costly. So, in most codes, it is accepted that the structure may undergo substantial deformations in the ALIE- yielding, plastic mechanisms, buckling are allowed, but the integrity of the structure with respect to global stability shall not be put in jeopardy.[8] For this kind of analysis, it is not natural to base the design on pressure-area relationships because the ship will not simply crush the ice. The pressure experienced in a collision depends on the relative resistance of the ship and icebergs and the motion excited. This can only be assessed accurately if both the ship and the ice are modelled and if the interaction between the two structures is taken into account.[8]

Integrated analysis of ship-bergy bit ice impact is done in this thesis work, where both the resistance of ship and ice is considered. A large passenger ships, which has IB ice class, is used to contact with ice floe. The objective is to see what kind of damage on the ship structures can be caused by impacting with ice floe.

Chapter 3

Review of IACS Ice Rules

Although it is not explicitly stated, the conventional design of ship structures is carried out in the ULS format. This also stays true for design of ice going ships. The rules for ice going ships are mainly:

- IMO:Polar Code and EEDI (Energy Efficiency Design Index). The polar code will come into force in 2017, and contain requirements on: Stability, Subdivision and Emergency Systems. EEDI is related to Environment Protection.

- Classification Society rules: Classification societies give rules for structural integrity.

- National Rules (Finish Swedish rules and NSR rules): The Finnish- Swedish ice class rules are aimed to Baltic operations, but used as industry standard for first year ice. The Northern Sea Route (NSR) rules are mostly concerned with operational issues (icebreaker escort, ice pilots).

All classification societies, except Russian Register, have adopted the IACS ice classes. The content and background theory of IACS polar class rules will be discussed below to shed some light on the design of ice going ships nowadays. The derivation of design ice load is shown.

3.1 Brief review of IACS ice class rules

The Unified Requirements for Polar Class ships apply to ships constructed of steel and intended for independent navigation in ice-infested polar waters. The Polar Class (PC) notations and descriptions are given in figure 3.1. It is the responsibility of the Owner to select an appropriate Polar Class. The descriptions in Table are intended to guide owners, designers and administrations in selecting an appropriate Polar Class to match the requirements for the ship with its intended voyage or service.[2]

Polar Class	Ice descriptions (based on WMO Sea Ice Nomenclature)
PC 1	Year-round operation in all polar waters
PC 2	Year-round operation in moderate multi-year ice conditions
PC 3	Year-round operation in second-year ice which may include multi-year ice inclusions.
PC 4	Year-round operation in thick first-year ice which may include old ice inclusions
PC 5	Year-round operation in medium first-year ice which may include old ice inclusions
PC 6	Summer/autumn operation in medium first-year ice which may include old ice inclusions
PC 7	Summer/autumn operation in thin first-year ice which may include old ice inclusions

Figure 3.1: Polar Class [2]

The hull of Polar Class ships is divided into areas reflecting the magnitude of the loads that are expected to act upon them. In the longitudinal direction, there are four regions: Bow, Bow Intermediate, Midbody and Stern. The Bow Intermediate, Midbody and Stern regions are further divided in the vertical direction into the Bottom, Lower and Icebelt regions. The extent of each hull area is illustrated in Figure 3.2. [2]

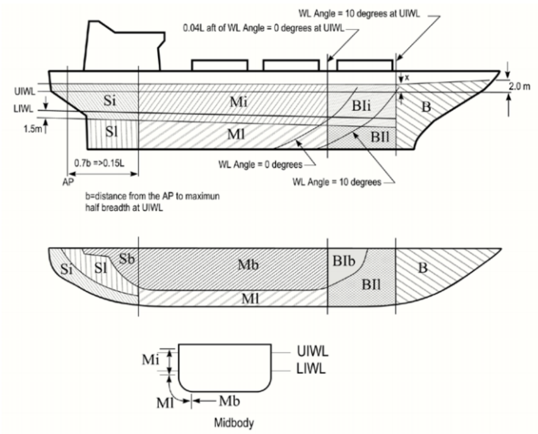

Figure 3.2: Hull area [2]

The design scenario is a glancing impact on the bow area[4], and the design ice load for the bow area is described directly in the rules. For other area indicated in the figure, there is a Hull Area Factors (shown in Figure 3.3) defined in the rules that reflects the relative magnitude of the load (compared to the bow area) expected in that area. The Hull Area Factor shows the pattern of the distribution of ice load along the ship hull. Bow and Bow intermediate area is expected to have higher load than Mid body and Stern. Then, the requirements toward the shell thickness and framing are specified based on the design ice load.

Hull area		Area	Polar Class						
			PC1	PC2	PC3	PC4	PC5	PC6	PC7
Bow (B)	All	B	1.00	1.00	1.00	1.00	1.00	1.00	1.00
Bow Intermediate (BI)	Icebelt	BI_i	0.90	0.85	0.85	0.80	0.80	1.00*	1.00*
	Lower	BI_l	0.70	0.65	0.65	0.60	0.55	0.55	0.50
	Bottom	BI_b	0.55	0.50	0.45	0.40	0.35	0.30	0.25
Midbody (M)	Icebelt	M_i	0.70	0.65	0.55	0.55	0.50	0.45	0.45
	Lower	M_l	0.50	0.45	0.40	0.35	0.30	0.25	0.25
	Bottom	M_b	0.30	0.30	0.25	**	**	**	**
Stern (S)	Icebelt	S_i	0.75	0.70	0.65	0.60	0.50	0.40	0.35
	Lower	S_l	0.45	0.40	0.35	0.30	0.25	0.25	0.25
	Bottom	S_b	0.35	0.30	0.30	0.25	0.15	**	**

Figure 3.3: Hull Area Factors [2]

The polar class rules have requirement toward the structure of ship for several aspects, which are:

- Design ice loads: It serves as a basis for scantlings design below. The design ice load is characterized by a design load patch, with uniform average pressure. It is dependent on the displacement of ship, chosen ice class and hull shape. With a higher class, the load is also higher.

- Shell plate thickness: It is dependent on the orientation of the framing, frame spacing, Hull shape, Material strength and the design ice load.
- Framing: There are different rules toward different type of frame. The requirement is toward the actual net effective shear area and actual net effective plastic section modulus.
- Material: There are requirement toward the steel grade.
- Longitudinal strength: A ramming impact on the bow is the design scenario for the evaluation of the longitudinal strength of the hull. Ice loads are only to be combined with still water loads.

The design ice load is discussed in detail below, because it is more related to this project. The discussion will focus on the idea in the background theory.

3.2 Design Ice Load

The design scenario in IACS Ice Class rules is glancing collision with an ice edge (edge of a channel, edge of a floe) on the shoulders of the bow. The ice load model assumes a 'normal' type of impact, in which the collision is idealized as a one-dimension impact.[4] Claude Daley extended Popov's method to several interaction geometry cases, and it is served as the foundation for Design Ice Load part in IACS Polar Class Rules.

Ice forces on ships and structures are typically the result of collisions[4]. Ice collision forces can be determined by energy considerations[4]. The force is found by equating the normal kinetic energy with the ice crushing energy.[4]

$$KE_n = E_{crush} \tag{3.1}$$

The crushing energy is found by integrating the normal force over the penetration depth.

$$E_{crush} = \int_0^\delta \mathrm{F_n}(\delta)\,\mathrm{dx} \tag{3.2}$$

The normal kinetic energy combines the normal velocity with the effective mass at the collision point

$$KE_n = \frac{1}{2} M_e V_n^2 \tag{3.3}$$

Where:

δ: Normal ice penetration during the impact.

F_n: Normal force

M_e: Effective Mass

V_n: Normal velocity

To solve F_n, it is firstly necessary to solve KE_n. The normal velocity is quite clear, which is dependent to the design speed of the vessel and also the hull shape at the collision point. The design speed is assumed to be class dependent. However, the effective mass defined is quite complicated and the idea behind it is not easy to see. Based on the formula, the Effective Mass is a function of inertia properties, hull angles and main dimensions.

After getting the expression of KE_n, a function relates the F_n to δ need to be formulated to solve the equation. Depending on the interaction geometry, there should be a relation between the ice penetration and contact area. With this penetration-area relation, if there is also a relation between contact area and pressure, then the function relates ice penetration and normal force can be constructed.

There are several models for the average pressure developed. The earliest one was proposed by Korzhavin, in which the ice pressure assumed to be uniform on the contact area and assumed to be proportional to the uniaxial compressive strength of ice.[14] For ship applications, Kurdiumov and Kheisin developed a concept based on the observed flow of crushed ice from the contact zone. The next development in modeling the ice pressure was the observation that the ice pressure seems to vary in general terms with area. Some of the ship based measurement results are plotted in Figure 3.4. It is actually hard to explain this observed pressure-area relationship. However, combining this observed area-pressure relation, the energy equation can be solved. The pressure-area function has a form shown below.

$$P = P_0 A^{ex} \tag{3.4}$$

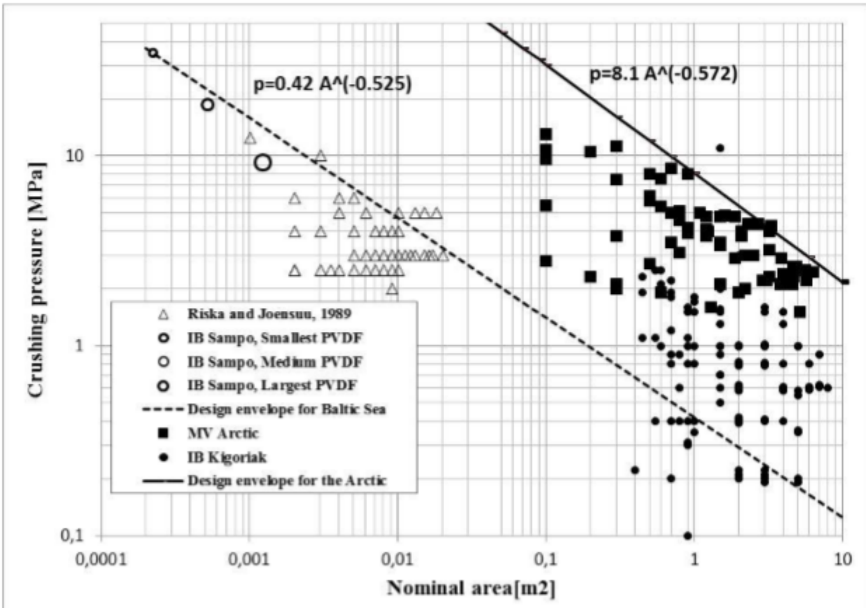

.

Figure 3.4: Avearge pressure measured on different contact areas in ship tests [14]

The general idea in the Claude Daley's energy method is shown above.It is quite easy to use it to get the design ice load, but some parts of this method are not well justified. Firstly, the contact force should be limited by the ice strength, if it is assumed that the ship will crush the ice without deformation (the ship strength is beyond consideration). But in the method, there is no part related to the ice strength. The pressure-area relation may represent the ice material property in some extent, but this relation itself has too many uncertainties and not justified. Besides, the energy to be dissipated by the crushing energy in not defined clearly. The design scenario is described as: the ship penetrates the ice and rebounds away. So the energy to be dissipated by the crushing energy should be the difference between the initial kinetic energy and kinetic energy at the maximum contact force. But it is actually calculated by combining the normal velocity and 'effective' mass at the collision point. The effective mass is defined by thinking that the collision point will accelerate because of the collision. The corresponding inertia mass is defined as the effective mass. But from the formula to calculate the effective mass, it is hard to see its connection with the definition.

The method to get design ice load discussed above only considered the crushing case. But in most case, the ice fails by bending. The flexural failure will limit the ice load. The bending resistance of ice is related to the ice thickness, ice flexural strength and hull angle, which determines the force angle. The ice thickness and ice strength are assumed to be class dependent.[4]

The above discussion has shown how the force can be calculated anywhere on the bow. To continue with the design the load patch must be found. The nominal contact area is found from the pressure-area relation. The load patch is assumed to have a rectangular shape. This is because it is convenient to do structural analysis based on this load. A reduction in the size of the load patch is introduced to account for the typical concentration of force that takes place as ice edges spall off.

The conclusion in this part is that, the method to calculate the design ice load in IACS ice class rules is based on simplified method, and the pressure-area relation of ice material is a key point in the method. The pressure-area relation of ice material represents the material behaviour of ice in some extent. The design principal is that the ship will crush the ice, so that the design ice load is dominated by the resistance of ice. Then the ship structures are designed to resist the maximum pressure from ice load.

Chapter 4

Introduction of External Mechanism

In the ALS design, it is convenient to split the collision scenarios into external mechanics and internal mechanics. It simplifies the numerical simulation of collision. The external mechanism is introduced in this part.

In ship-iceberg collision, the action is characterised by the kinetic energy. The kinetic energy can be determined on the basis of relevant masses, velocities and directions of ships. A part of the kinetic energy will remain as kinetic translation or rotation energy after collision, but the other part needs to be dissipated as strain energy from the deformation of both ship and iceberg.

The external mechanics deals with rigid body motions and determines the energy to be dissipated as strain energy. It actually considers the global translational and rotational momentum balance for the ship and iceberg. But how this dissipated energy is distributed between striking and struck part, which is dependent on the relative strength of two parts, is not a concern in external mechanism. Solving the external mechanism provides a perspective about how much the extent of the deformation in structures should be.

Experience has shown that ship-iceberg impacts produce considerable motion in the components yaw and roll due to eccentricity.[9] In particular, if the collision happens at the bow of a ship, the shape of the outer shell is not a vertical wall and it has a significant influence on the final dissipated energy.[9] If only 3DOF(2D) is taken in to account, then the vertical eccentricity and excited roll motion of ship are not considered, which may lead to an overestimate of the dissipated energy. Thus, modelling a ship and iceberg collision should take the 6DOF into account for each object involved. [9]

Zhenhui Liu has developed a new formulation for the analysis of the external mechanics of ship collisions that can be applied to both 2D and 3D cases. A briefly review of his paper and discussions regarding a case study in his paper is made below. The objective here is to show what External Mechanism can deal with.

4.1 Literature Review: new formulation of the impact mechanics of sihp collisions and its application to a ship-iceberg collision

In his paper, a fully 3D solution to the ship collision problem is proposed based on Stronge's work. The basic assumptions in Stronge's theory are[16]:

- The impact duration is short, and the impact force is large, so all other external forces are neglected.
- The deformations are limited to a small area within the contact surface.

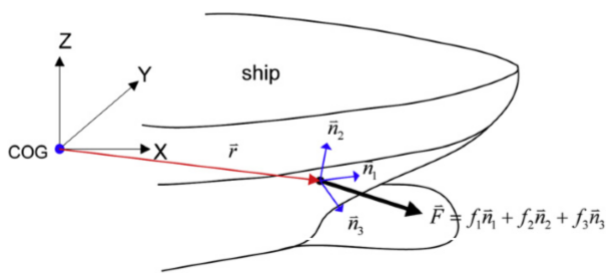

Figure 4.1: Collision point geometry and local coordinate system,modified from Daley [3]

Generally, the ship motions are described in the global coordinate system XYZ as shown in the figure 4.1. However, in Stronge's impact mechanics, a local coordinate system is established to derive the equations of motion. The local coordinate system is established with respect to the common tangent plane at the contact point.

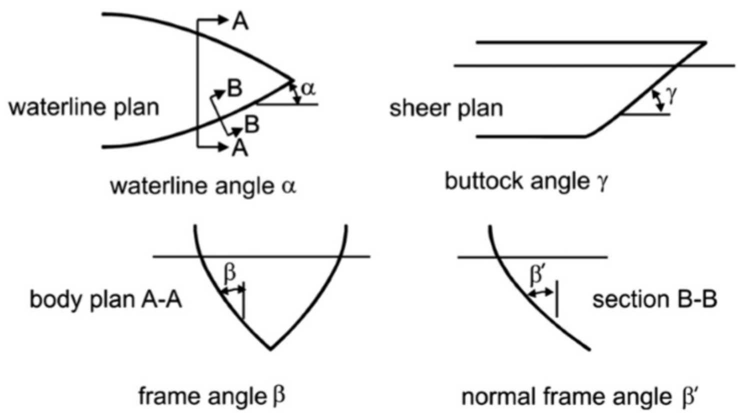

Figure 4.2: Definition of hull angles [9]

Thus, a transformation matrix from global coordinates system to local coordinate system need to be established. The transformation matrix is established based on the hull angles defined by DNV; see Fig.4.2

- α: waterline angle
- β: frame angle
- β' normal frame angle
- γ: sheer angle

The formulas related to the Stronge's impact theory and the derivation of dissipated energy in 6DOF is quite complicated, so they are not introduced here. For more information, refer to paper [9]

Pedersen and Zhang developed an impact mechanics model of ship-ship collisions, which is only valid for the 3DOF(2D) case. The 6DOF(3D) impact mechanics formulated by Zhenhui Liu can be degraded to the 2D expressions. So Zhenhui Liu analysed a ship-ship collisions case the same with Pedersen and Zhang's using his method and compared the results.

Two identical supply vessels are sailing with a forward speed of 4.5m/s. Collisions take place with different impact angles and locations; see Fig. 4.3. The length of each vessel is 82.5 m, the breadth is 18.8 m, the draught is 7.6 m, and the

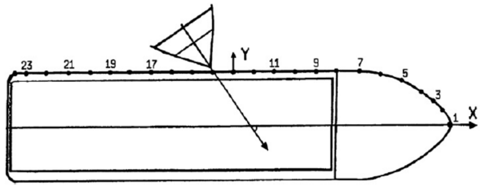

Figure 4.3: Illustration for the case study [13]

displacement is 4000 t. The radius of inertia for yaw motion is 20.6 m. The added mass coefficients are the same as those used in the original paper.

Zhenhui Liu degrade his method to 2D and analysed this ship-ship collision case and get excellent agreement with the result from Pedersen and Zhang, as shown in figure 4.4. It is worth noting that the energy ratio normally gets it maximum value for midship. The reason for this is that little yaw motion is excited, so very little energy is transferred to rotational kinetic energy. However, collisions with θ equal to 120 and 150 follow a different trend because of velocity component in Y direction is very small, so very little yaw motion is excited. When the collision takes place forward of 0.2d/L in these two cases, the collision becomes increasingly similar to a head-on collision.

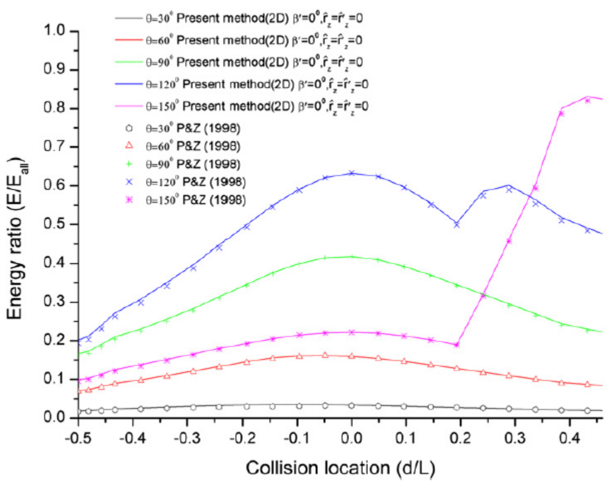

Figure 4.4: Comparison of 2D numerical simulations [9]

Zhenhui Liu has also analysed this case in 3D. In the 2D analysis, vertical

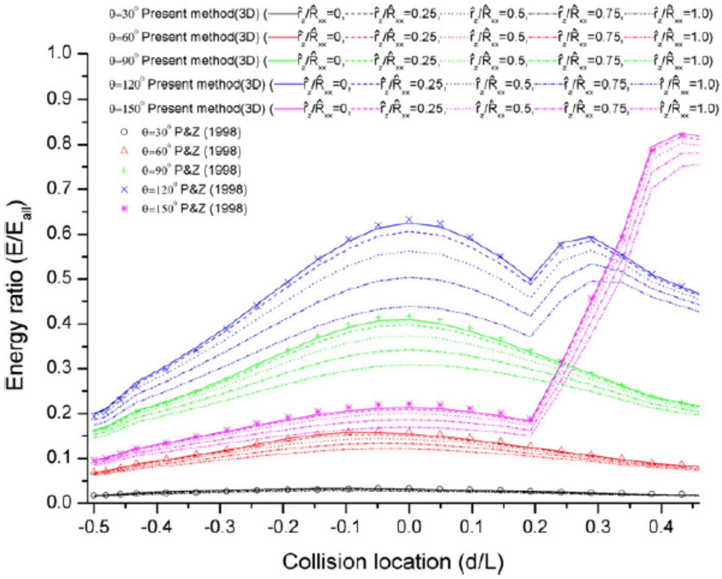

Figure 4.5: 3D numerical simulations [9]

eccentricity was not considered. When it is taken into account, the roll motion of the ship can be excited. The results of the 3D analysis are presented in figure 4.5. It is interesting to see that the vertical eccentricity has a more significant influence on the dissipated energy for amidships than stem and stern. This is because for stern and stem, the excited roll motion is shadowed by the relative larger yaw motion.

Chapter 5

Introduction of Internal Mechanism

Solving the external mechanics only gives the energy to be dissipated in strain energy in ship and iceberg, but how this energy is distributed is still unknown. This problem is solved in Internal Mechanism. There are three design strategies to deal with this problem with respect to the relative deformation between striking and struck part: strength, ductility and shared energy design.

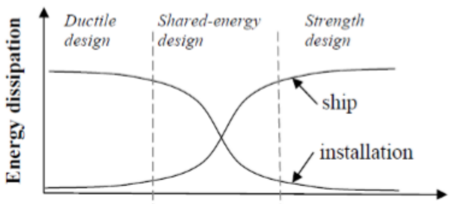

Figure 5.1: Relative Strength [7]

- Strong design - the ship is strong enough to resist the collision force with minor deformation, this force the iceberg to deform and dissipate the major part of the collision energy.
- Ductility design - the ship undergoes large, plastic deformations and dissipates the major part of the collision energy.
- Shared energy design - both the iceberg and the ship contributes to the energy dissipation and undergoes large deformations.

In strong design, the ship is actually seen as a rigid body, so it can crush the ice without deformation. In other word, the ship is not allowed to go over obvious deformations. This strategy will usually produce over strengthened ship which is too heavy and costly. In the ductile design, the ice is actually seen as a rigid body, so the ship will take most part of the dissipated energy and have large deformation. But in reality, the ice will actually have considerable deformation and even be crashed, so this ductility strategy overestimate the Ice load. The share energy design is actually more reasonable because it considers the deformation both in ship and ice. The internal mechanism here corresponds to the share energy design in ALS design stage, which consider the deformation of both ship and iceberg.

Because of the large deformation, Non-linear finite element methods are always used to analyse the internal mechanics.[8]. The non-linear finite element code LS-DYNA 971 was used to assess deformation of both the ship structure and the iceberg. To do a Non-linear finite element analysis, firstly FE models of the ships and iceberg should be created, which can represent the geometry and material behaviour appropriately. Zhenhui Liu has developed a model of an ice-strengthened FPSO structure and a sphere shape iceberg model in his paper.[8] A brief review of the models he created and later the results from the simulation in LS-DYNA is discussed below.

5.1 Literature Review: Plasticity based material modelling of ice and its application to ship-iceberg impacts

5.1.1 Ship model

In the simple linear elastic simulation, in which the steel material model was regarded as isotropic elastic material obeying Hook's Law, Young's Modulus and Poisson's ratio is enough to define the material model. But in NLFEA, yielding, hardening and fracture also need to be taken in to consideration, so a more complicated material model is needed to describe the material behaviour accurately.

The model created by Liu was assumed to have isotropic plastic properties and the yield surface is Von Mises yield surface. The material is in elastic domain if:

$$\sigma_{eq} < \sigma_y \tag{5.1}$$

The 'power law' relationship was used to simulate the stress-strain plastic behaviour. The equivalent stress-strain relationship is represented by a modified power law formulation that includes the plateau strain:

$$\sigma_{eq} = \begin{cases} \sigma_y & \text{if } \epsilon <= \epsilon_{plat} \\ K(\epsilon_{eq} + \epsilon_0)^n & \text{if otherwise} \end{cases} \tag{5.2}$$

where:

equivalent stress

$$\sigma_{eq} = \sqrt{\frac{3}{2} s_{ij} s_{ij}} = \sqrt{3J_2} = \\ \sqrt{\frac{(\sigma_{11} - \sigma_{22})^2 + (\sigma_{22} - \sigma_{33})^2 + (\sigma_{33} - \sigma_{11})^2 + 6(\sigma_{12}^2 + \sigma_{23}^2 + \sigma_{31}^2)^2}{2}} \tag{5.3}$$

ϵ_{plat}: equivalent plastic strain at the plateau exit

σ_y: initial yield stress

ϵ_0: given by $\epsilon_0 = (\frac{\sigma_y}{K})^{\frac{1}{n}} - \epsilon_{plat}$

During the collision, the ship shell may be penetrated by the ice, so it is necessary to simulate the formation of fracture and crack of steel. The RTCL damage criterion was employed so that steel fracture and crack can be captured in the simulation. If the element failed this damage criterion, it will then be removed.[1] The RTCL criteria may be expressed mathematically as:

$$\dot{D} = \begin{cases} 0 & T < -1/3 \\ \frac{\sigma_1}{\sigma_{eq}} \dot{\epsilon_{eq}} & -1/3 <= T < 1/3 \\ exp(\frac{3T-1}{2}) \dot{\epsilon_{eq}} & \text{otherelse} \end{cases} \tag{5.4}$$

$$D = \frac{1}{\epsilon_{cr}} \int \dot{D} dt \tag{5.5}$$

Where:

$T = \sigma_m / \sigma_{eq}$ σ_m is the hydrostatic stress.

D: describes the rate of damage, element is deleted if it's value exceed 1

σ_1: major principal stress.

ϵ_{eq}: rate of the equivalent plastic strain.

ϵ_{cr}: critical equivalent plastic strain in uniaxial tension.

5.1.2 Ice model

There are lots of uncertainties to define the shape of iceberg. But it is not really necessary to define the overall shape of icebergs because only the shape at the contact area has influence to the impact. Two different iceberg shape are proposed by Liu. The first one is a sphere with a radius of 2000 mm and the second is composite shape comprising a sphere of radius 1000 mm in the front, a rounder platform of height 2000 mm and top and bottom radii of 1000 mm and 1500 mm respectively. (see Figure 5.2)

In particular, small icebergs may have small sections that protrude out of the main body. In principle, such protrusions may penetrate deep into the side structure and ultimately tear open the inner shell.[8] The second ice model with a smaller nose radius of 1000mm were chosen to shed some light on this issue.

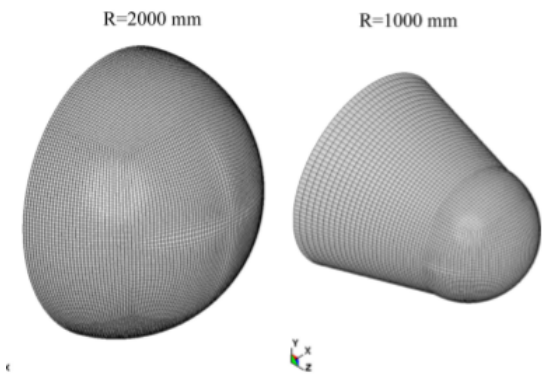

Figure 5.2: Proposed iceberg shapes [8]

The material model for the iceberg is based on the 'Tsai-Wu' yield surface developed by Liu, Løset and Amdahl. The ice material model is introduced more in detail in the Ice Mechanism Part.

5.1.3 Simulation Results

The response of the ship and iceberg can be formally represented as load-deformation relationships, as illustrated in Figure 5.3. The strain energy dissipated by the ship and iceberg equals the total area under the load-deformation curves. 'i' represents ice and 's' represents ship in the formula below.

$$E = E_i + E_s = \int_0^{w_{i,max}} R_i dw_i + \int_0^{w_{s,max}} R_s dw_s \tag{5.6}$$

It is possible to get the damage on ship structures after collison by combining the external and internal mechanism. First, by solving the external mechanism, the energy which should be dissipated as strain energy is got. And then use this load-deformation curve from internal mechanism to get the deformation of ship corresponding to the dissipated energy. Which is worth noticing is that R_i andR_s should equal to each other corresponding to Newton's third law, so there is only one solution existing.

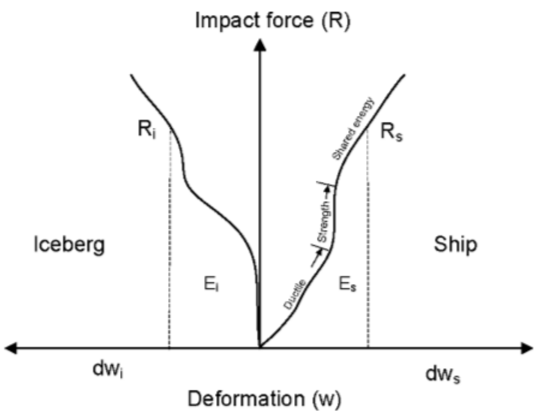

Figure 5.3: illustration of the load-deformation curve between the iceberg ans ship [8]

How the dissipated energy is distributed is influenced by the relative strength of the striking and struck part. The energy dissipation tend to be distributed to the weaker of the two parts. Liu adjusted the relative strength of ship and iceberg to research on this effect. The most logical way to adjust the relative strength of the iceberg and the ship is to either change the ship scantling or let the ice material parameters vary. As the ice material has been calibrated to test data, changing the material parameters would introduce additional uncertainties. Changing the scantlings of the ship side is cumbersome.[8] So Liu adjust the ship strength by simply scaling the yield strength. The load-deformation curves for five different ship strength cases are plotted in figure 5.4. As it is shown in the figure, with smaller ship strength, the ice behaves more like a rigid body with less deformation.

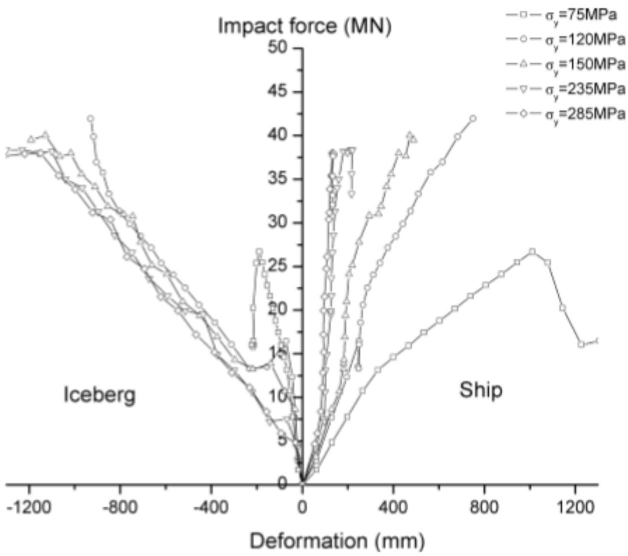

Figure 5.4: Load-deformation curves for 5 different yield stress of ship material [8]

The shape of the iceberg can also influence the distribution of dissipated energy significantly. Iceberg with small protrusions may even penetrate the deep into the side structure and ultimately tear open the inner shell.[8]. Liu proposed a method to quantify the influence from the shape of iceberg. He thought that the shape of iceberg can be considered according to the structural configuration. He proposed to use aspect ratio to describe the shapes of the leading edges of icebergs. The aspect ratio is defined as:

$$A_r = \frac{H}{D} \tag{5.7}$$

Where:

D: Equal to the spacing between strong structure components in a ship, such as stringers, frames, deck, or bulkhead.

H: Determined as illustrated by figure 5.5.

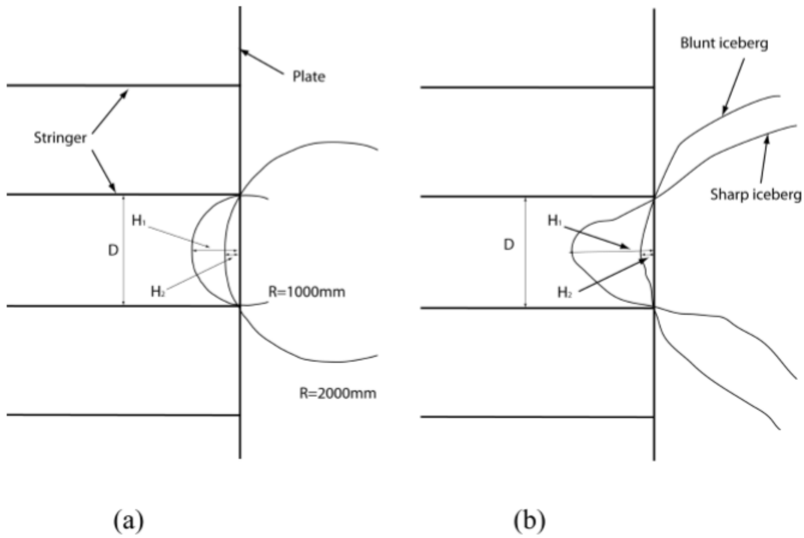

Figure 5.5: Illustration of aspect ratio definition for(a) a sphere and (b) arbitrary shaped iceberg profiles [8]

It is reasonable to guess that, if D is an constant, with higher aspect ratio, the ice model possess more potential to penetrate the shell.

Chapter 6

Mechanical and Physical properties of ICE

To get an accurate integration analysis for accidental iceberg impact, in addition to iceberg mass and speed, iceberg shape, a continuum-mechanics model of iceberg is required. Ice material model for Finite Element Modelling is previously not well established, but in Liu's paper, a simple plastic model is proposed which seems to describe the ice material model well.

Iceberg ice falls within the category of a multi-year ice,which has survived at least two summer seasons. It is composed of freshwater ice from land-based glaciers flowing off the land into the sea. Iceberg ice can be idealised as an isotropic material, as it shows no significant different mechanical properties in each direction. In this sense, it is comparatively simpler than sea ice.[10] However, iceberg ice is also influenced by temperature, porosity, grain size, strain rate and confinement. In general the ice becomes weaker and softer with increasing temperature, porosity and grain size. Strength increases with increasing strain rate until brittle failure takes over after which strength decreases. There exists a transition from ductile to brittle, with a strain rate of 10^3.[10] In iceberg collisions, it is believed that the strain rate is greater than the transition value. Basically, the strain-stress behaviour of ice is strain rate and temperature dependent.[10]

Ice is a very complicated material, so it is not reasonable to try to establish a model which can describe the ice material behaviour exactly. The criterion of Liu's ice model is that: if the model with simple inputs is capable of predicting reasonable pressure-area relationships in the case of Strength design, it is considered to be sufficiently accurate to be used in Shared-energy design. The ice model established by Liu is introduced below and then the test to verify this model is discussed.

6.1 Introduction of the Ice Material Model

In general, to establish a material model, it is actually necessary to determine several aspects of the material listed below:

- Yield criterion: It states that when the yield begins. In triaxial stress state, the yield criterion is always expressed by a yield surface. The state of stress inside the yield surface is elastic. When the stress state lies on the surface the material is said to have reached its yield point and the material is said to have become plastic.
- Hardening Rule: It describes how the yield criterion is changed by the history of plastic flow.
- Elastic Modulus, Poisson's ratio: They describe the stress and strain relation before yield.
- Flow Rule: It leads to a relation between stress ans strain after yielding.
- Erosion: It simulates the material failure.
- Density: In the collision analysis, the density is important because it is related to the kinetic energy.

Among this material properties, the Elastic Modulus and Poisson's ratio can be got from uniaxial tensile testing, since the iceberg can be idealized as an isotropic material. And in Liu's ice model, the ice is assume to be elastic-perfect plastic, so there is no need to establish a flow rule. Hardening rule is also not necessary because the nature of ship-iceberg action is transient. So, only the yield surface and Erosion is established, and they are shown below.

In the case of iceberg impact, ice particles in center contact area are significantly confined from neighbouring particles, which means that the ice is in a triaxial stress state.[10] In this sense, triaxial experiments should be carried out prior to

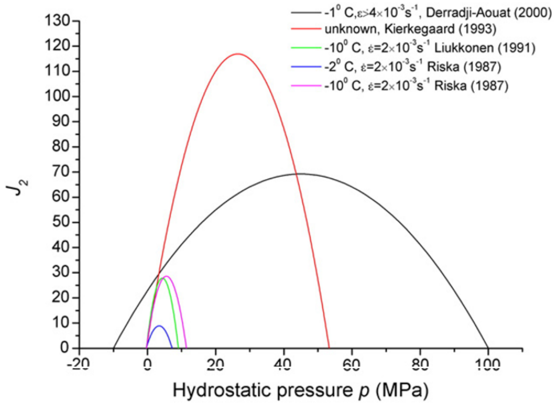

Figure 6.1: Illustration of Tsai-Wu yield surface in $p - J_2$ space [10]

Items	Derradji-Aouat (2000)	Kierkegaard (1993)	data 1 by Riska and Frederking (1987)	data 2 by Riska and Frederking (1987)
Constant a_0	22.93	2.588	1.60	3.1
Constant a_1	2.06	8.63	4.26	9.20
Constant a_2	−0.023	−0.163	−0.62	−0.83

Figure 6.2: Input parameters for the iceberg material model [10]

adopting a suitable yield surface. In Liu's ice model, the Tsai-Wu yield surface is used, which has form shown below. Figure 6.1 shows a comparison of the recommended inputs based on various data sources in $p - J_2$ space. It is seen that there are big differences existing which are due to the different data sources and the fitting methods used to approach the experimental data sets. The input parameters for the iceberg material model is shown in Figure 6.2.

$$f(p, J_2) = J_2 - (a_0 + a_1 p + a_2 p^2) = 0 \tag{6.1}$$

where:

a_0, a_1, a_2, are constants that require curve fitting to triaxial experiment.

$p = \frac{\sigma_{kk}}{3}$, is the hydrostatic pressure.

J_2 is the second invariant of deviatoric stress tensor.

The influence from temperature and strain rate toward this yield surface is then analysed. Løset has performed a comprehensive study on the temperature profile of icebergs. This study found that for icebergs at sea, there is a temperature gradient from the surface to the core region due to the low thermal conductivity of ice.[11] The corresponding change in the yield surface can be considered in the following way:

$$f(p, J_2) = J_2 - (a_0(T) + a_1(T)p + a_2(T)p^2) = 0 \tag{6.2}$$

Where T is the temperature. Linear interpolation is used for the elements between the surface and the core area.

The strain rate dependence has not been incorporated into the present model, because the lack of experimental data makes it impractical to consider the strain rate in the material model. Instead, a yield surface represents high strain rates is used in the following numerical simulations.

The common way to simulate failure is to use erosion technique. Elements violating the failure criterion are deleted. An empirical failure criterion based on effective plastic strain and hydrostatic pressure is proposed by Liu.

$$\epsilon_{eq}^p = \sqrt{\frac{2}{3}\epsilon_{ij}^p : \epsilon_{ij}^p} \tag{6.3}$$

$$\epsilon_f = \epsilon_0 + (\frac{p}{p_2} - 0.5)^2 \tag{6.4}$$

Where:

ϵ_{eq}^p: equivalent plastic strain

ϵ_{ij}^p: plastic strain tensor

ϵ_0: initial failure strain

p_2: larger root of the yield function

ϵ_f: failure strain

if $\epsilon_{eq}^p > \epsilon_f$ or the pressure is not greater than the cut-off pressure p_{cut}, erosion is activated. The cut-off pressure describes the ice strength in tensile, while the failure strain represents the ice strength in compression. This failure criterion is based on trial and purely empirical. Only one input parameter (ϵ_0) is needed, and it should be adjusted according to experimental data.

6.2 Verification of the Ice Material Model

Liu has then conducted several numerical simulation to verify this ice material model in LS-DYNA. The result of the numerical simulation is presented below to show this Ice Material Model works.

The first case simulates iceberg collision with rigid wall. This case concerns a conically shaped iceberg colliding with a rigid wall. During crushing, the pressure-area relationship is recorded. Various yield surface have been used shown in Figure 6.1. Figure 6.3 shows the recorded maximum contact pressure versus contact area based on various yield surface inputs. The design curve proposed by Masterson et al.(2007) is plotted for comparison, which is also recommended by the ISO code. This comparison shows that the yield surface derived by Derradji-Aouat(2000) and Kierke-gaard(1993) produces values closet to the pressure curve recommended by ISO/CD 19906(2010), when the contact area is less than $0.5m^2$.

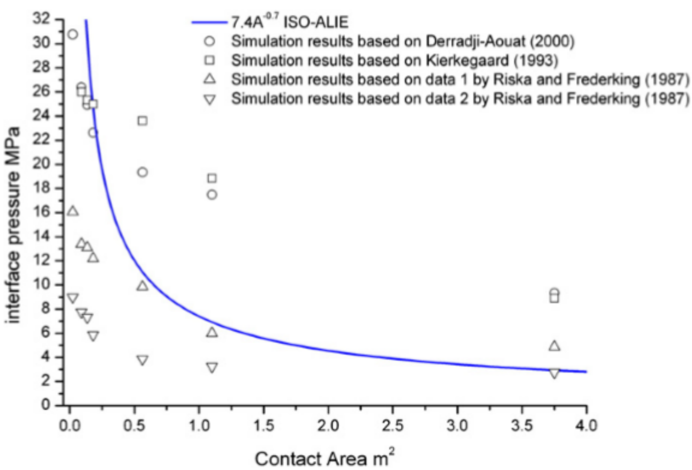

Figure 6.3: Recorded Maximum contact pressure versus contact area [10]

Liu also used this ice material model to simulate the ship-iceberg collision. A ship bow-iceberg head-on collision scenario is carried out in order to investigate features of the material model. Collision between ship bow and iceberg wall and also rigid wall is simulated. The model established is shown in Figure 6.4.

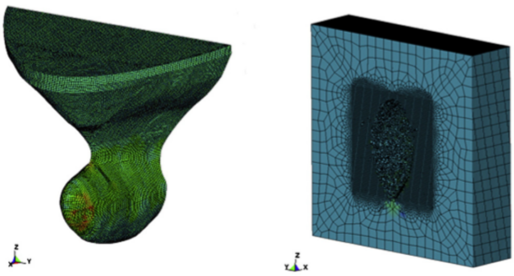

Figure 6.4: Bow and iceberg wall model [10]

The penetration versus internal energy is shown in Figure 6.5.

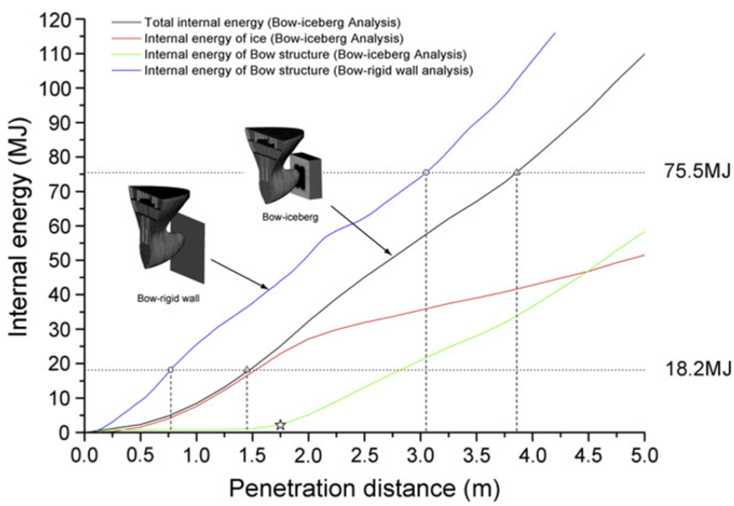

Figure 6.5: Internal energy versus penetration distance [10]

Figure 6.5 shows that the strain energy is dissipated in both the iceberg and the ship structure for the bow collision with iceberg. If the dissipated energy can be got from External mechanism, then it can be inserted into the figure as total internal energy and the corresponding internal energy in ship bow and iceberg can be found. The maximum dissipated energy corresponds to a central plastic impact, the value can be calculated based on the formula proposed by Liu and Amdahl.[9]

$$E_0 = \frac{1}{2} M_{iceberg} v_{ship}^2 \frac{(1 - \frac{v_{ice}}{v_{ship}})^2}{1 + \frac{M_{iceberg}}{M_{ship}}} \tag{6.5}$$

Because of eccentricity of the contact force, the dissipated energy is usually smaller than the maximum dissipated energy from central plastic impact. Then the dissipated energy can be calculated either involving a energy ratio or establish 3D solution introduced in external mechanism part.

The two simulation shows that the ice material model established by Liu yields good result. It undergoes mesh convergence and the computational time is acceptable.[10]. The material model is successfully applied to simulation of ship bow-iceberg collisions.

Chapter 7

Software Introduction

Two software are used in this project, which is Msc. Patran and LS-DYNA. Below is a brief introduction of these two softwares.

7.1 Msc. Patran

The geometry modelling and meshing are done in the finite element software MSc. Patra. Patran is a powerful finite element modelling software, with different possibilities of modelling and meshing advanced geometry. Patran does also include tools for computing mass, radius of gyration and centre of gravity. Based on the FE modelling, input files for analyses in a lot of different FE solvers can be written, and in this thesis input files for LS-DYNA are created.

7.2 LS-DYNA

LS-DUNA is a general purpose finite element code for analysing the larege deformation static and dynamic response of structures including structures coupled to fluids. Full theory is described in LS-DYNA theory manual and some of the important factors are described below.

7.2.1 Time integration

LS DYNA is a computer program using the explicit central difference scheme to integrate the equations of motion.[17] To illustrate this integration method, an example of single degree of freedom damped system is shown below.

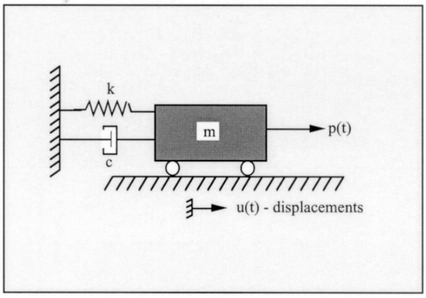

Figure 7.1: Single degree of freedom damped system [17]

The equation of motion is:

$$m\ddot{u} + c\dot{u} + ku = p(t) \tag{7.1}$$

Central difference scheme is an explicit method, for which the equation of motion is evaluated at the old time step t_n.[17]

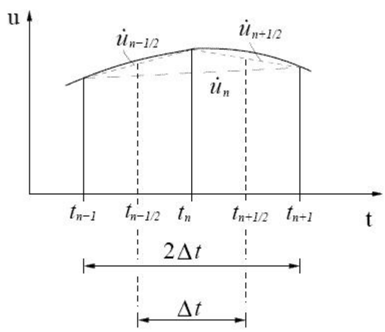

Figure 7.2: Centaral Difference

Velocity:

$$\dot{u}_n = \frac{1}{2\Delta t}(u_{n+1} - u_{n-1}) \tag{7.2}$$

Acceleration:

$$\begin{aligned} \ddot{u}_n =& \frac{1}{\Delta t}(\dot{u}_{n+\frac{1}{2}} - \dot{u}_{n-\frac{1}{2}}) \\ =& \frac{1}{\Delta t}(\frac{u_{n+1} - u_n}{\Delta t} - \frac{u_n - u_{n-1}}{\Delta t}) \\ =& \frac{1}{(\Delta t)^2}(u_{n+1} - 2u_n + u_{n-1}) \end{aligned} \tag{7.3}$$

Equilibrium at time t_n:

$$M\ddot{u}_n + C\dot{u}_n + Ku_n = P_n \tag{7.4}$$

Substitute equation (7.2)and(7.3) into equation (7.4)[17]:

$$(M + \frac{1}{2}\Delta tC)u_{n+1} = \Delta t^2 P_n - (\Delta t^2 K - 2M)u_n - (M - \frac{\Delta t}{2}C)u_{n-1} \tag{7.5}$$

The time integration loop used in LS-DYNA is found in LS DYNA Support , as shown in Figure 7.3.

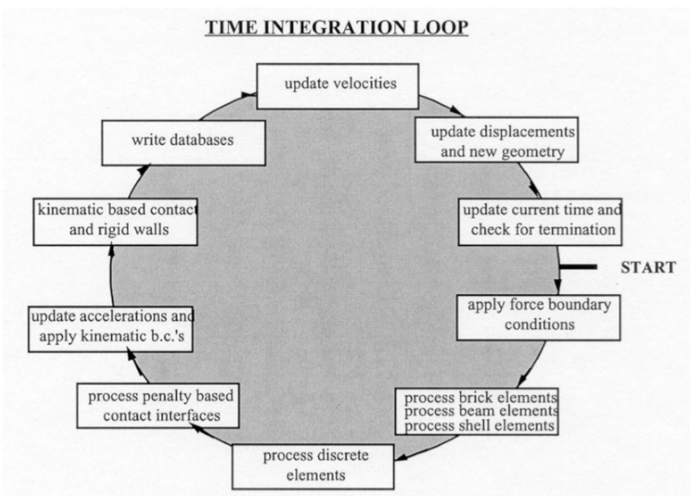

Figure 7.3: Time integration loop in LS-DYNA[17]

7.2.2 Integration stability

For FEA the time cost is usually the governing factor. The time step size is limited by the smallest element in the finite element mesh. To fulfil the stability conditions, the time step needs to be smaller than the time it takes the pressure wave from the impact to pass the element. If the time step is too large, the pressure wave will pass uncontrolled and cause the structure to become unstable.[17]

For shell elements, the critical time step size is given by:

$$\Delta t_c = \frac{L_s}{c} \tag{7.6}$$

Where Ls is the characteristic length of an element and c is the sound speed in the material given by:

$$c = \sqrt{\frac{E}{\rho(1-\upsilon^2)}} \tag{7.7}$$

where E is the Young's Modulus, ρ is the specific density of the material and υ is Poisson's ratio.

7.2.3 Contact-Impact algorithm

The treatment of impact and sliding along interfaces has always been an important capability in LS-DANA.

Contact is defined by identifying where to be checked for potential penetration[12]. Contact treatment is internally represented by linear springs between the slave nodes and the nearest master segments. Penalty-based approach is the default method and uses the size of the contact segment and its material properties to determine the contact spring stiffness. As this method depends on the material constants and the size of the segments, it works effectively when the material stiffness parameters between the contacting surfaces are of the same order-of-magnitude. A search for penetrations is made every time step. When a penetration is found, a force proportional to the penetration depth is applied to resist and ultimately eliminates the penetration.[5]

Contact Type

To enable flexibility for the user in modelling contact, LS-DYNA presents a number of contact types and a number of parameters that control various aspects of the contact treatment. Some points while choosing the contact types are listed below:

- 'Automatic' type: Automatic contact types are non-oriented, meaning they can detect penetration coming from either side of a shell element. When the surface orientations are known through the analysis, the non-automatic contact types may be effective. In crash analysis, the deformations can be very large and predetermination of where and how contact will take place may be difficult or impossible. For this reason, the 'automatic' contact options are recommended.

- One-way treatment of contact: 'Master' surface and 'Slave' surface is defined. Only the user-specified slave nodes are checked for penetration of the master segments. For example: CONTACT_AUTOMATIC_ NODES_TO_ SURFACE.

- Two-way treatment of contact: The subroutines which check the slaves nodes for penetration, are called a second time to check the master nodes for penetration through the slave segments. The treatment is symmetric and the definition of the slave surface and master surface is arbitrary since the results will be the same. For example: CONTACT_SURFACE_TO_SURFACE

- 'Single' type: These contact types are the most widely used contact options in LS-DYNA. No master surface is defined. Penetration is checked between all the parts in the slave list, including self-contact of each parts. If the model is accurately defined, these contact types are very reliable and accurate. However, if there is a lot of initial penetration, energy balances may show either a growth or decay of energy as the calculation proceeds. Note that the most common contact related output, RCFORC(Contact force), is not written for single surface contacts, since the net force is zero.

- Tied contact: In tied contact types, the slave nodes are constrained to move with the master surface.

Contact Parameters

There are several contact-related parameters in LS-DYNA that can be used to modify or, in many case, improve contact behaviour. The main contact parameters are described below.[17]

- Sliding Friction: Contact sliding friction in LS-DYNA is based on a Coulomb formulation. Friction is invoked by giving non-zero values for the static and dynamic friction coefficients.

- Penalty Scale Factors: Penalty scale factors provide a means of increasing or decreasing the contact stiffness. The default values generally work well for contact between similarly refined meshes of comparably stiff materials. For dissimilar mesh size and material, non-default values penalty scale factors may be necessary to avoid the breakdown of contact.

- Contact Thickness: Allow users to directly specify the desired contact thickness. Sometimes this item is used to decrease the contact thickness and thus eliminate initial penetrations.

Initial Penetration

Initial penetration is a term used frequently to describe the amount of penetration that exists between a node and its closest master segment or between two interacting segments during the initialization of the problem. This initial force can in some instances be very large which may have adverse effects on the stability of the model. These forces could also lead to localized initial stresses and strains that may be non-physical. Additionally, if the penetrations were unable to be removed completely at the first cycle, they tend to be carried over to the subsequent cycles leading to a ‘negative energy‘ condition altering the numerical accuracy of the simulations.[17]

The most obvious recommendation would be to have no initial penetrations at all. However, this is rather difficult due to the nature of the model building process. Some recommendations for treating initial penetration are listed below.[17]

- Default Treatment: When a slave node is found to penetrate its closest master segment, LS-DYNA updates the nodal coordinates to remove the penetration without applying any force. By setting IGNORE=2 in CONTROL_CONTACT, LS-DYNA write the list of offending nodes and their initial penetration values into D3HSP file.

- Contact thickness scaling: Scaling of contact thickness, which has no effect on the structural thickness specified in the section definitions.

- By setting IGNORE=1, the initial penetration is noted and compensated by adjusting the contact thickness locally.

Contact Energy

There are energy involved during the impact process. LS-DYNA will output the energy data, and the energy balance can be used to check numerical result in some extent. The energy balance in general can be written as:

$$\text{Total Energy} = \text{Initial Total Energy} + \text{External Work} \tag{7.8}$$

Or in other words, the energy ratio is equal to 1.0.

$$\text{energy ratio} = \frac{\text{total energy}}{\text{initial total energy} + \text{external work}} \tag{7.9}$$

The total energy reported in DATABASE_GLSTAT consists of different types of energy, which are introduced below.[17]

- Internal energy : The energy dissipated by strain energy in striking and struck part. It includes elastic strain energy and work done in permanent deformation. It is computed in LS-DYNA based on the six components of stress and strain. The internal energies of all the elements is summed to give the total internal energy.

- Kinetic energy: The energy remained as kinetic energy during the impact.

- Contact(sliding) energy: Include slave energy, master energy and friction energy. The slave/master energy is a function of penetration and contact force. They indicate the energy needed to prevent penetration. If the friction is 0, slave and master energy should be close in magnitude but opposite in sign. Large or negative contact energy is a sign for concern. When friction is included in contact definition, positive contact is to be expected. Abrupt increase in negative contact energy may be caused by undetected initial penetrations.

- Hourglass energy: To overcome 'Shear locking' behaviour, FE software offers reduced integration schemes, which use less points than required for exact integration. This leads to better numerical results for some types of behaviour as the stiffness is reduced. But unfortunately, reduced integration induces other unwanted behaviours, hourglass issue. The stiffness matrix is formed by integration at the reduced Gauss points. If the FE model is loaded in such a way that the nodal displacements cause no strain at the Reduced Gauss points, then that mode of displacement will induce no strain energy in the element and therefore the element will have no stiffness to resist this load. With full integration, there are no such hourglass modes. To check the hourglass level, one should compare it with the internal energy. Hourglass energy should not exceed 5 percent of internal energy.

- System Damping energy: Damping energy is associated with the energy dissipated by damping.
- Eroded energy: Eroded energy is the energy associated with deleted elements.

7.2.4 Criterion of Numerical Simulations with good Quality

Some criterion of accurate numerical simulation in LS-DYNA are proposed by Martin Storheim in his doctoral thesis.[15].The criterion are listed below:

- The energy ratio should be close to 1.(requires that all energy components are included in CONTROL ENERGY.)
- Check that the ratio of hourglass/internal energy is less than 10 percent for every part.
- Check that the sliding energy is positive and the sliding energy is far lower than the internal energy.

Martin Storheim also proposed some suggestions of how to deal with negative sliding energy and large hourglass energy. They are listed below:[15]

Method to deal with negative sliding energy:

- Check and eliminate initial penetration.
- Check for and eliminate redundant contact conditions.
- Reduce the time step scale factor
- Set contact controls back to default except set SOFT=1 and IGNORE=1 (Optional Card C).

Method to deal with large Hourglass energy:

- Refine the Mesh
- A pressure loading is preferable than loading over node
- Use full integration. But this may induce too stiff structure.

Chapter 8

NLFEA Modeling

This master thesis work involves lots of modeling work. The procedure to create the FE model for both ship and ice floe is illustrated in this chapter. The setup for the impact analysis is also introduced here.

8.1 Ship Model

The ship model used in this master thesis project is MS Color Magic, which is a cruiseferry owned and operated by the Norway-based shipping company, Color Line, on their route connecting Oslo, Norway to Kiel, Germany. The scantlings and ship drawings are provided by Professor Jørgen Amdahl. Main dimensions for the ship is shown in Table. Some drawings of the ship are shown in figure 8.1-8.3.

Tonnage	75100 GT/ 4750 DWT
Length	224m
Beam	35m
Draught	6.8m
Speed	22knots(41km/h)
Capacity	2700 passengers

Table 8.1: Main Dimensions of the MS Colour Magic

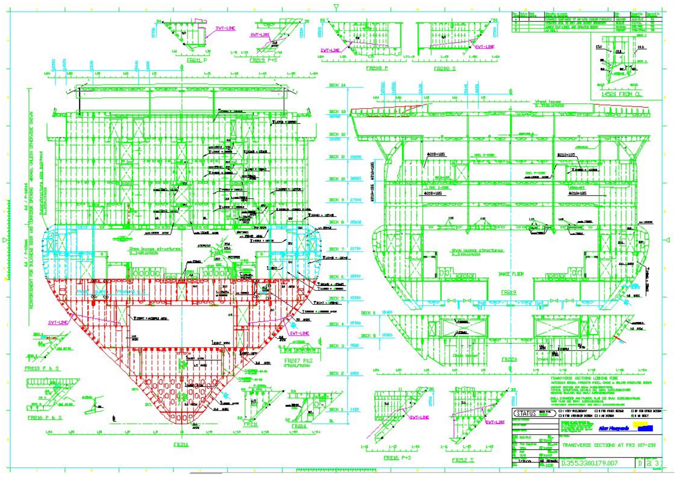

Figure 8.1: Fr210,220 Transverse Sections

Figure 8.2: Deck 3

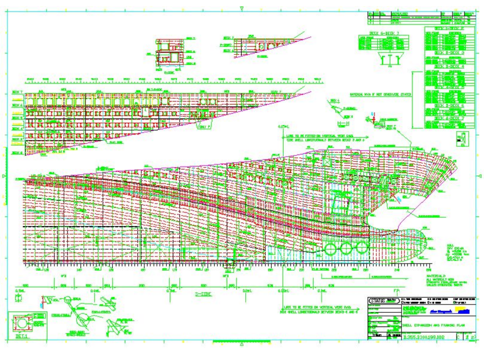

Figure 8.3: Shell Expansion

8.1.1 Geometry Model

The ship-iceberg collision normally happens in the bow and shoulder area. Since the ship will always be operated to prevent from head-on impacting at bow, so the impact location is determined at the shoulder area. In order to reduce the simulation and modelling time, only the impacted tank is modelled. The tank should be large enough compared with the ice floe. Appropriate boundary condition should be applied to simulate the end of the tank.

Fr205 to Fr230 of the ship is modelled. The length of the model is 20.9m. Only half of the ship about center line is modelled because of the symmetry. Appropriate boundary condition is introduced at the center line section to simulate the interaction between the two half parts. Considering the ship-iceberg impact normally happens around the waterline, only the part between base line and deck 5 is modelled. This is an ice classed ship and the part between deck 2 and deck 3, which is around the waterline, is the ice strengthen area. At this area, the shell plate is thicker and the frame is arranged for per half frame space.

Because this is at the shoulder area of the ship, the shape of the transverse sections are changing rapidly along the longitudinal direction. To capture the shape of the ship accurately, the ship lines data are read for each half frame from the waterline drawings listed above. Due to insufficient transverse section drawings, some ship lines are estimated to make the surface as smooth as possible. The ship lines of each transverse section, which are smoothed in AutoCAD, are shown in figure 8.4.

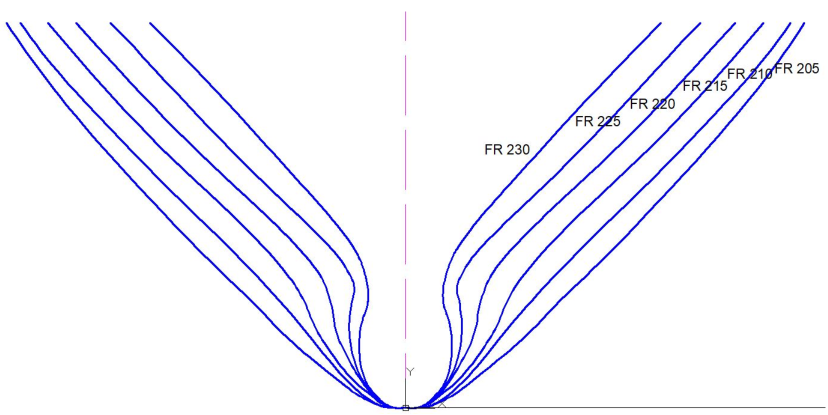

Figure 8.4: Smoothed Ship Lines in AutoCAD (Only 5 transverse sections are shown)

The geometry model is made in Patran. Firstly the shape line of each half frame is created, using the data of the smoothed line in AutoCAD. The surface is then created between each line to get the side shell of the ship. The frame in both longitudinal and transverse direction is then added on the side shell. The 5 decks are created then at the their specific heights. Longitudinal and transverse bulkheads are then added between each deck. At last, the longitudinal and vertical stiffeners and girders are then added on decks and bulkheads. The size of the stiffeners, girders and frames are changed a little bit at the connection point with deck or side shell, to avoid very sharp elements later during mesh.

One key point in building geometry model is that any two intersecting surfaces must share one line at their border, so that they can share nodes after meshing. Sharing nodes means they are connected to each other in reality. This has been done for almost all intersecting surfaces in the model, except for the intersection between transverse web and longitudinal stiffeners on the deck. See Figure 8.5. So the longitudinal stiffeners just pass through the web, like there is a hole cut in the web. But the hole is also not modelled, since it will involve too much modeling work. It is shown later that this inaccuracy will cause some initial stress in the model.

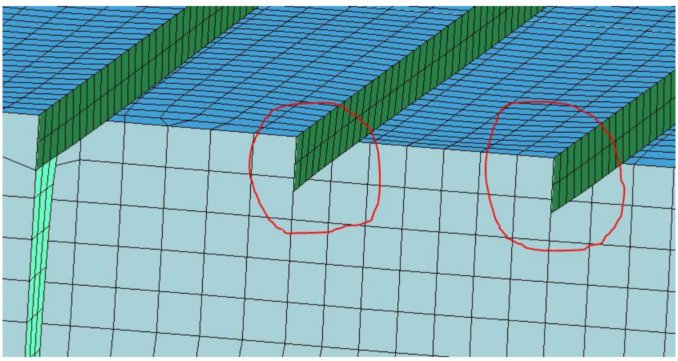

Figure 8.5: Inaccuracy Modeling: Stiffeners passing through Transverse Web

The thickness of each part is then added as section properties, based on the shell expansion drawings shown above.

The coordinate system is arranged so that the x-axis is in the ship transverse direction, the y-axis is in the ship longitudinal direction, and the z-axis is in the vertical direction. The geometry model in Patran environment is shown in figure 8.6.

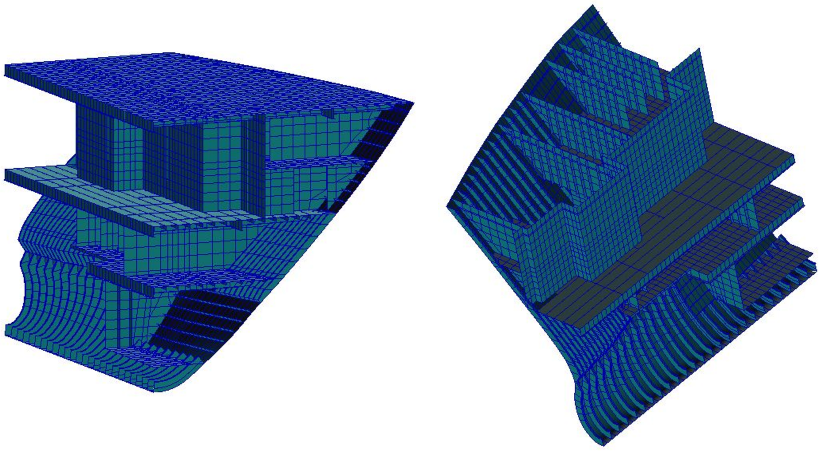

Figure 8.6: Geometry Model of the Ship Structures in PATRAN

8.1.2 Meshing

The geometry model is then meshed in Patran. For most regular areas, for example the deck area near center line, Quad4 shell elements are used. The elements seems to have a good aspect ratio. However, at some irregular areas, such as the deck areas near the ship side, or at the connection point with vertical stiffeners on bulkhead, triangular elements are used to adapt to the irregular geometry or to connect the parts. See figure 8.7. The triangular elements are highlighted by green color. The element size is usually selected as 10 times the plate thickness. The mean thickness of this structure is around 10mm, so 100mm is chosen as the mean element size. Because of the irregular shape. it is difficult to make all elements 100mm. After quality check of the mesh. The largest element are thought to be 220mm. The smallest elements are thought to be 26mm. The simulation time will be affected by the smallest element size in a large extent. Too small element will cause very long simulation time, which is not the case in this simulation. Element with very sharp angles is avoided, because it can bring fake stress concentration. The total number of Quad4 elements in the ship structure reaches 236751. The number of triangular elements is 1910.

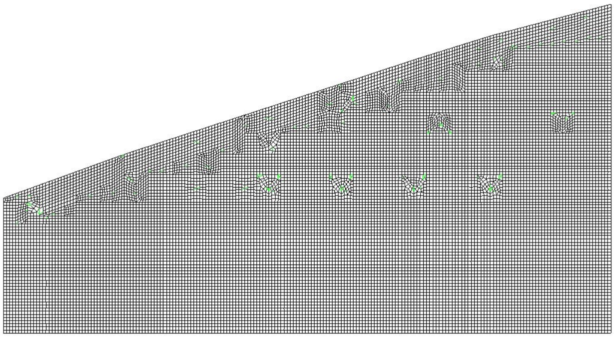

Figure 8.7: Mesh of Deck 5

8.1.3 Material Model

After completing the geometry model in Patran, the model is transferred into LS-Dyna Prepost to set the material property. RTCL damage criterion combined with the power law material model is used for the steel of the ship structure. The RTCL damage criterion and power law material model is introduced in Chapter 5. The material properties is not set exactly as mentioned in the drawings of the ship. That is because the accurate property parameters of the material mentioned in the drawings were not found. But in the drawings, it has stated that for side shell structures, high strength steel is used, so in alternative, the material property which represents high strength steel is used for most simulations. Mild steel is used for one simulation to see what happens if the relative strength of ship structures is reduced. The material property for the steel of the ship is listed in table 8.2 and 8.3.

Table 8.2: Material Parameters for High Strength Steel

Item	Value
Yield stress E	$338MP_a$
Strength index K	$728Mp_a$
Young's modulus E	$204GP_a$
Poisson's ration ν	0.3
Density ρ	$7.85e03kg/m^3$
Strain Index n	0.16

Table 8.3: Material Parameters for Mild Steel

Item	Value
Yield stress E	$275MP_a$
Strength index K	$800Mp_a$
Young's modulus E	$210GP_a$
Poisson's ration ν	0.3
Density ρ	$7.85e03kg/m^3$
Strain Index n	0.16

8.2 Ice Model

Comparing to the ship model, it is much easier to build the ice model due to its simple geometry. It is not necessary to capture the exact geometry of the entire ice floe, but the geometry of the part, which impacts with ship shell, needs to be taken into consideration. To reduce the simulation time, the rear part of the ice, which is far from the contact area is replaced by rigid material. The density of the rigid part is condensed to get desired mass of the entire ice floe.

8.2.1 Geometry Model

Two geometries are selected for the ice model. The first one has cylinder geometry with diameter 10m and 1.2m thickness. The thickness is chosen according to FINNISH SWEDISH ICE CLASS RULES. This ship has IB ice class, which corresponds to a level ice with thickness not exceeding 0.6m. The thickness is multiplied by 2 to consider potential rafting of Multi-year ice. The second one has a cone combined with half a cylinder. This geometry is selected to have a sharper edge impacting with the side shell, in order to have some penetrations on the side shell. The top project view of the two models and 3D geometry model is shown in figure 8.8.

The ice model is divided into an ice part and a rigid part. Ice material is used for the ice part, but rigid material is used for the rigid part. These two parts share nodes at their boundaries. The size of the rigid part is shown in figure 8.8. The rigid part is far from the impact location, so it will have little influence on the result. By doing so, with less elements using ice material, the simulation time will be reduced significantly.

8.2.2 Meshing

The ice model is also created in PATRAN. Firstly, the 2D cross section of the models are created and meshed. The mesh size is selected the same as the ship structures, which is 100mm. Then the 2D shell elements are extruded along the axis to get the 3D FEM model, which is composed of solid elements, as shown in figure 8.9. Ice material is used for the blue part, but rigid material is used for the grey part.

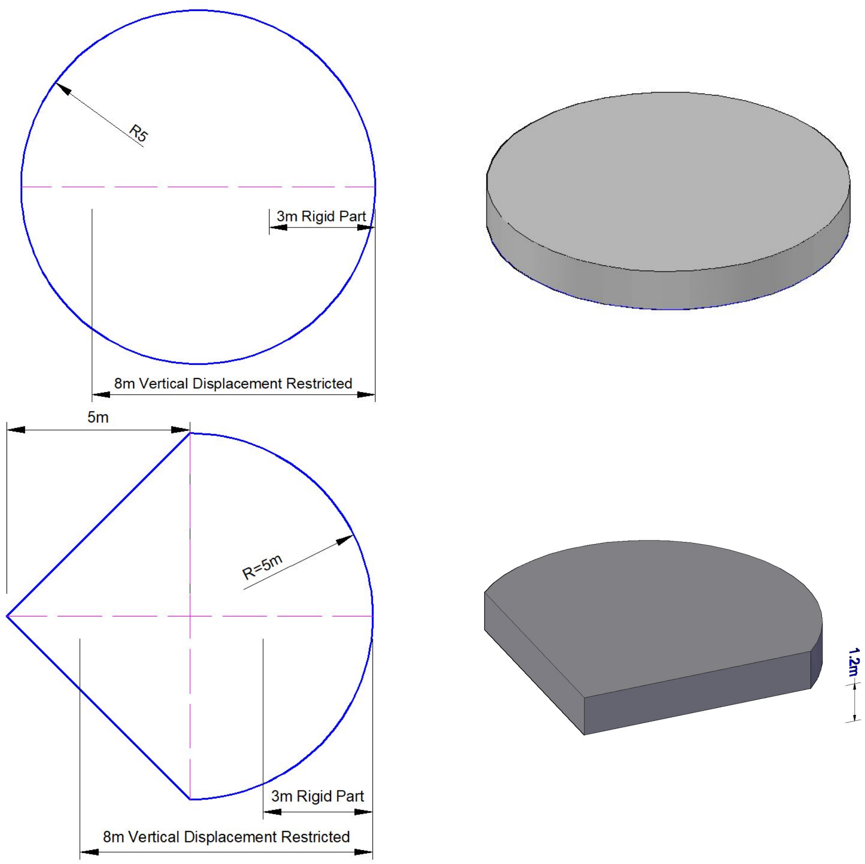

Figure 8.8: Geometry Model of the Ice

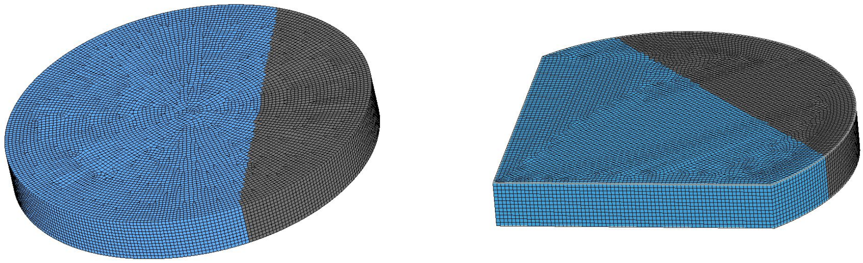

Figure 8.9: FEM Model of the Ice

8.2.3 Material Model

Then, Liu's ice material model is introduced for the ice part. This ice material model is introduced in chapter 6. The material parameters are shown in table 8.4. This one represents the Multi year ice, which is composed of fresh water. The Multi-year ice is stronger than the normal sea ice. It is more difficult to be crushed.

Table 8.4: Material Parameters for Multi-year Ice

Item	Value
constant a_0	$22.93Mp_a^2$
constant a_1	$2.062.06Mp_a$
constant a_2	-0.023
Initial failure strain ϵ_0	0.01
Young's modulus E	$9.5GP_a$
Poisson's ration ν	0.3
Density ρ	$900kg/m^3$

8.3 Pre-processing

The pre-processing for the analyses is done in LS-Prepost. Boundary conditions introduced, contact area defined, initial velocity added and termination time given. There are also other options, which control the simulation process, are set to have a good numerical quality. They are described below. The model in LS-Prepost environment is shown in figure 8.10.

8.3.1 Boundary Conditions and Collision Positions

Only part of the ship is modelled, so appropriate boundary conditions should be introduced to compensate for the non-modelled part. The nodes in the two ends transverse surface and longitudinal center surface are fixed against move in all degree of freedoms. The ship structure was big enough to minimize the influence of the boundary on the results. After the simulation, it can also be observed that the part, which is far away from the collision but close to boundary, has very stress developed. This may prove that the fixed boundary condition is appropriate. There is another boundary condition introduced for ice model. This is presented later.

The collision position is firstly set around the ice strengthen area, and at the center in longitudinal direction. Then one other location, which is above the ice strengthen area is selected to see what happens if the ice floe hits the weak area.

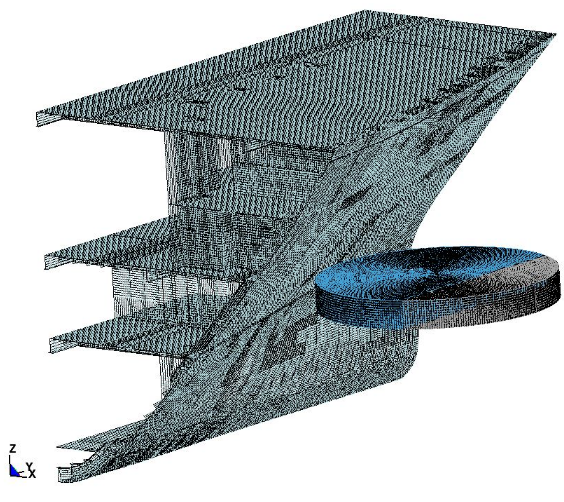

Figure 8.10: Pre-processing in LS-Prepost

8.3.2 Contact Definition

Three different types of contact are defined. CONTACT_Eroding_ Surface_to_ SURFACE was used to simulate the contact between ship shell and ice. This type of contact can simulate the solid elements erosion of the ice model. CONTACT_AUTOMATICAL_SINGLE_SURFACE was used for the ship self contact. CONTACT_ERODING_SINGLE_SURFACE was used for the contact inside ice. There is no need to define contact between rigid part and ice part, because they share nodes.

Friction is also introduced in the contact definition. The friction ratio is set to be 0.3 between steel structures, and 0.15 between steel and ice.

8.3.3 Initial Velocity and Termination Time

The speed of the ship is around 11m/s. But the contact location is at the shoulder area, so the contact speed should be only a fraction of the sailing speed. The drifting of ice floe can increase the contact speed. 6m/s is chosen to be the initial velocity of the ice model. This initial speed involves enough energy either to cause considerable deformation on the ship or crushing of the ice, and also produce acceptable simulation time. From several trial simulations, the actual calculating time is set to be 0.65s, which is enough to either stop the ice completely or crushing of the ice.

8.3.4 Other Options Controlling the Simulating Process

There are lots of options provided in Ls-Dyna Prepost for the users to adjust to get numerical results with good quality. It really takes time to comprehend the meanings and functions of these options. Some important options are introduced here. The important part of the input file in LS-DYNA is shown by an example in Appendix I.

<u>IGNORE</u>
Ignore initial penetrations in the options of contact definitions. When setting ignore to 0, Ls-Dyna move nodes to eliminate initial penetrations in the model definition. But this may introduce some initial stress which is not physical. When setting Ignore to 1, Ls-Dyna allows initial penetrations to exist by tracking the initial penetrations, so that there will be no initial stress. In the ship model, there are some inaccurate parts, which may lead to initial penetration. See figure 8.5. But it is found in this thesis work that, while using new version solver, there is no initial stress while setting ignore to 1. But when old version solver (ls971_R51) is used,

the initial stress exists. But the old version solver is used, since this is the only solver that contains both RTCL and Ice Material Model.

SOFT

The initial penetrations are not eliminated when SOFT=2 is used, rather the initially penetrated location becomes the baseline from which additional penetration is measured. It's this additional penetration that produces contact forces. However, the initial stress cannot be eliminated by setting soft to 2 in this thesis work.

LMC This is an option that defines the number of constants in the user-defined material model. In the Ice material model developed by Liu, there are 10 constants, but LMC is set to 8 by mistake firstly. The last two parameters control the erosion of the ice, so in the simulations with this mistake, the ice cannot be crushed. The material constants have been checked over and over again, but finally it is found that the mistake is actually in LMC. But the results of these simulations are also presented in the last section in Chapter 9. It is recommended to pay attention of inputting this parameter.

Chapter 9

LS-DYNA Simulation Results

Several simulations are done and the results are presented in this section separately with discussion. For different simulations, different ice model geometry, ice material, contact locations and different mass was applied. Figure 9.1 gives a clear illustration of what has been used for different simulations. In section 9.4, there is an error in the ice material model, so that the ice is uncrushable. The results of different simulations are compared and analyzed in different sections.

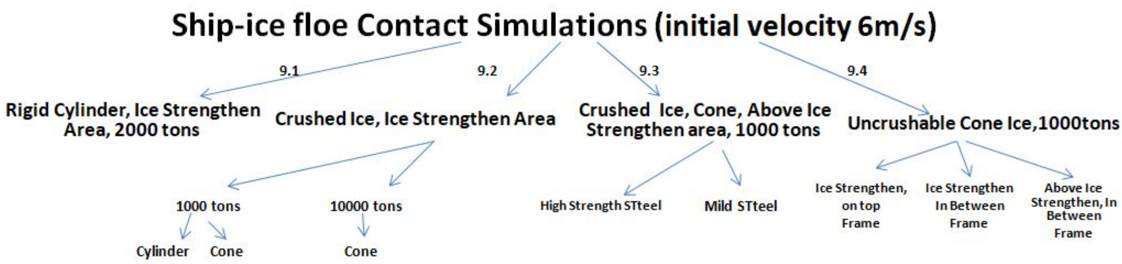

Figure 9.1: Illustration of all the Simulations (High strength steel is used except indication in section 9.3.)

9.1 Ship Structures Impact with Rigid Cylinder

Before introducing the ice material, it is interesting to research on the damage pattern of the ship structures. So a rigid cylinder was used to impact with the ship. The rigid body will not dissipate any energy, so it has the highest potential to damage the ship structures. After several trial simulations, the mass of the rigid cylinder is set to be 2000 tons, to produce obvious visual damage to the ship. The initial velocity is set to be 6m/s.

Figure 9.2 shows the final stage during the collision. It clearly shows that the ship is penetrated by the cylinder. The cylinder is removed to show the damage. In figure 9.3, the ship is cut at the most damaged cross section, to show the damage pattern more clearly. The cylinder was not stopped completely at last. But it is reasonable to speculate that it will not be stopped by the ship, since the ship structure has been damaged seriously with less capability to stop the ice. The velocity of the cylinder during the impact is shown in figure 9.4.

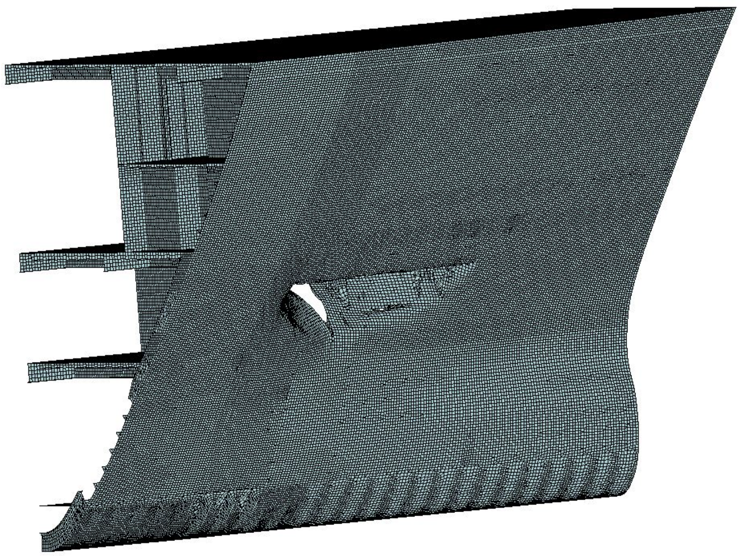

Figure 9.2: Damage of the ship at Last Time Step in the Simulation

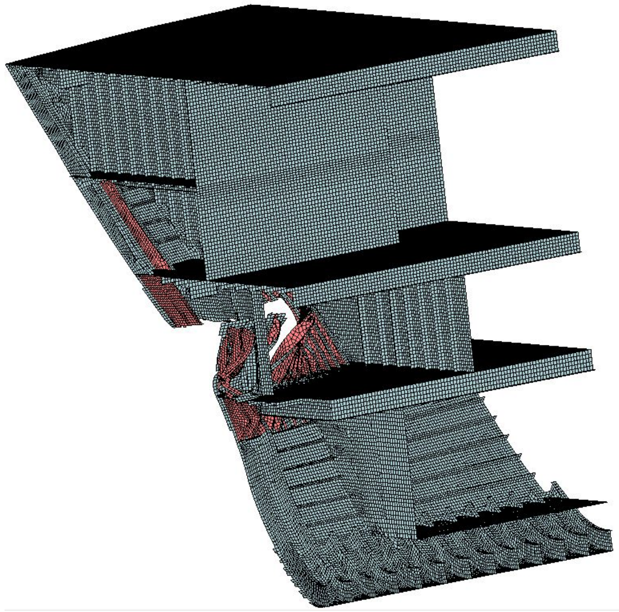

Figure 9.3: Most Damaged Cross Section

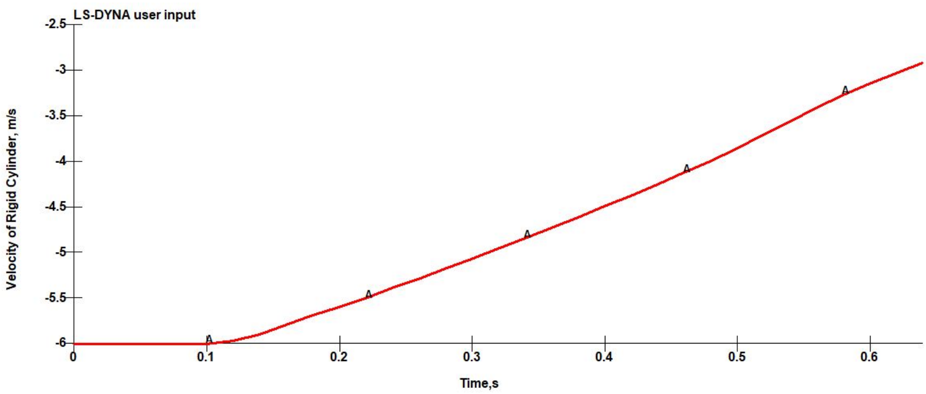

Figure 9.4: Velocity of the cylinder during the contact

Figure 9.5 shows the energy ratio during the collision. It is around 1 during the whole process, which represents a good energy balance during the simulation. Figure 9.6 shows the energy transferring. It clearly shows that the external energy (the kinetic energy of the cylinder), transfer to the internal energy (strain energy due to deformation), sliding energy (energy related to friction), and eroding energy (energy related to element deletion due to material failure criterion).

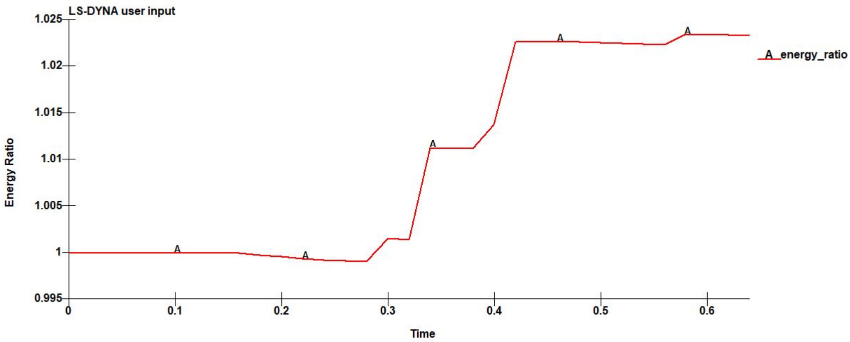

Figure 9.5: Energy Ratio during the contact

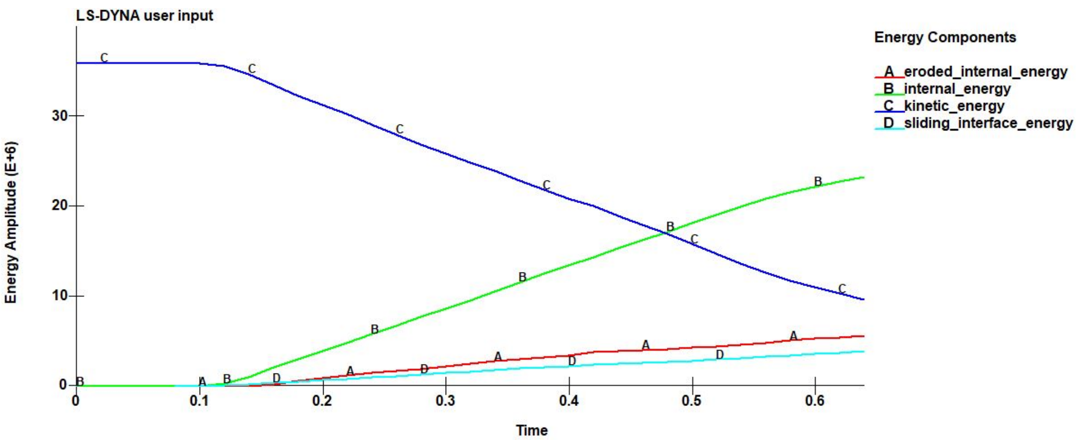

Figure 9.6: Energy transferring during the contact, Energy Unit: J

Figure 9.7 and 9.8(a) shows the cross section which is damaged most seriously. It shows that the top sharp edge of the rigid cylinder will hit the side shell firstly, and cause very high stress concentration there. Then it will tear up the side shell there and push the half bottom inward, until the other crack appears. This will cause huge deformation on the part of ship structure below the contact location. Due to huge axial force form the collision, the bottom deck will buckle a lot as shown in figure 9.8(a). But the part above the collision remains stable. That is because after crack appears, there is almost no contact between the rigid cylinder and the top half ship structure. So one conclusion here is that, due to the ship geometry, the collision with horizontal tough body will cause more damage to the structures below contact, if the shell is penetrated.

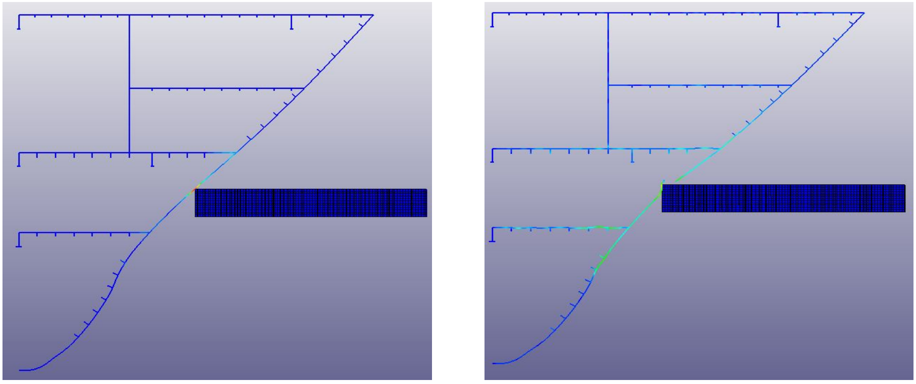

Figure 9.7: Most Damaged Cross Section

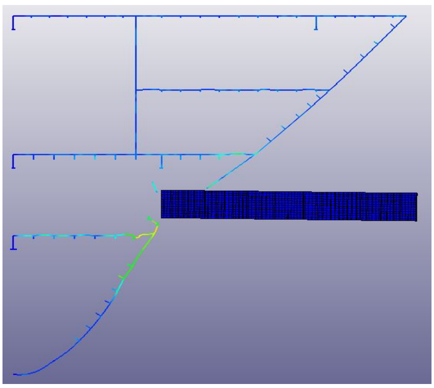

(a) Most Damaged Cross Section

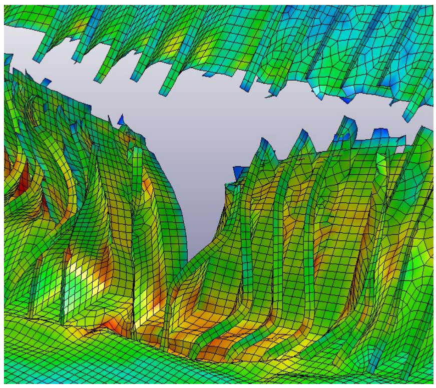

(b) Stress Distribution on Frames

Figure 9.8

Figure 9.9 shows the frame damage from inside perspective. It shows that there is no big overall deformation in the frame before crack appears. It means that the crack at the frame is also caused by high stress concentration. After the crack appears, the rigid cylinder will push the half bottom part inside rapidly, and this will cause lots of bending on the transverse frame. The ship structures don't have enough resistance to stop the rigid cylinder. But instead of in-plane bending directly, the transverse frame tends to be bent in out of plane direction, which has a much weaker bending resistance. Figure 9.8(b) shows the stress distribution on the frame. It shows that the highest stress appears at the end of the web. So if the rigid cylinder continues to go in, the fracture will appear at the end of the web firstly.

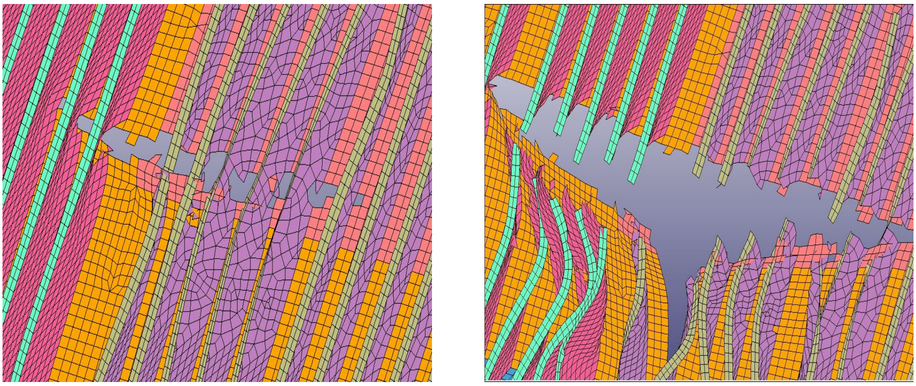

Figure 9.9: Frame Damage

The rigid cylinder penetrates the side ship shell very easily. That is because firstly the rigid cylinder is much more stiff than the ship structures. Then, the cylinder is rigid, so it will not deform at all. The contact area between the rigid cylinder and the ship side shell is thus so small that very high stress concentration appears at very small area. So cracks appears even there is no big deformation. The rigid edge of the cylinder cut the ship like a knife.

9.2 Ship Structures impact with Multi-year Ice Floe at Ice Strengthen Area

In this simulation, the Multi-year ice material is introduced. Two geometries are selected, which are shown in figure 8.8. The contact location is at the ice strengthen area and initial velocity of the ice is 6m/s. Density is given to the rigid part accordingly so that the entire model has mass of 1000 tons, which is the typical mass of bergy-bit ice or ice floe.

One extra boundary condition for the ice floe model is introduced in this simulation. The back 8m part of the ice model is restricted to move in vertical direction, as shown in figure 9.11. The reason for introducing this boundary condition is stated below. The edge of the ice will deform after contacting with the ship side shell. And because the side shell is inclined, so the contact force will push the ice downward, as indicated in figure 9.10. Besides, the friction between the ice and ship side shell is quite small, so that the ice will slip downward along the side shell instead of having real collision. But in reality, the existence of water will provide buoyancy force, drag force, and added mass force to support the ice, so the ice will not slip downward easily. However, there is no enough time left for simulating the interaction with water, so a simple boundary condition is introduced to prevent the ice from slipping downward. This assumed boundary condition is more critical, since it restricts the downward motion completely. But in reality, the ice will move downward finally, even though there is water to support it. Besides, the ice floe is always damaged by bending failure in reality, rather than crushed completely at the contact area. But the length of the cantilever is set so short, which is only 2m, that the ice will not be bent to failure. Which is worthy to mention is that 'slipping downward' is not a problem when only rigid body is used. That is because the rigid body will not deform so that the contact force will stay mostly in horizontal direction.

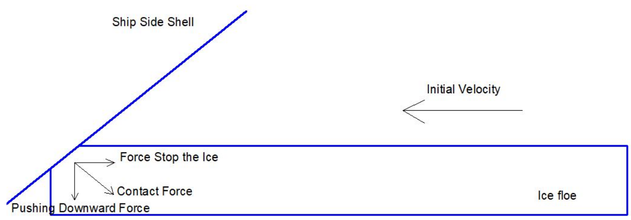

Figure 9.10: Deformed Ice pushed down by the Ship Structures

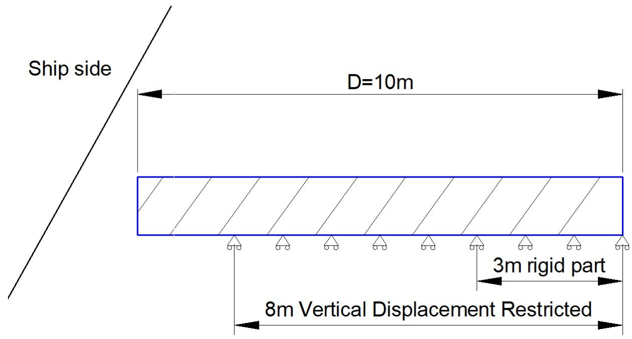

Figure 9.11: Extra Boundary Condition on Ice Model

The several items, which can be used to justify the simulation quality are listed in Appendix II and III. One criterion is violated. The sliding energy is positive while cylinder ice was used, but it is negative while cone ice was used. Sliding Energy should be equal to 0 if there is no friction between two contacting parts. It shouldn't be negative. The only difference in these two simulations is the geometry of the ice model, so the negative sliding energy shouldn't be caused by the initial penetrations in the ship model. It should relates to the erosion of elements, since in all the simulations without erosion, the sliding energy is positive. But the reason for why the cone shaped ice leads to negative sliding energy is not found.

The ice is crushed by the ship structures completely without causing much damage on the ship side. The resistance of the ship is very large compared to the ice floe. The crashed ice is shown in figure 9.13. Since the ice is crashed, the ice is only slightly stopped by the ship structures. The velocity of both ice geometries is shown in figure 9.12. It shows that the cylinder ice is stopped more than the cone ice. The reason is that there are more ice materials in the contact location for the cylinder ice, so there are more contact for the cylinder ice. The development of contact force also shows this pattern. As shown in figure 9.14, the contact force is higher for cylinder ice. The contact force shows a vibration pattern. That is because that the ice is crushed layer by layer, as shown in figure 9.13. The slope of the crushed cross section is due to the slope of the ship shell toward bow. The amplitude of the contact force goes up before the current layer of ice is crushed. It goes down when this layer is crushed. The amplitude of the contact force while crushing the next new layer is higher because the cross-section is bigger, so the contact area is bigger.

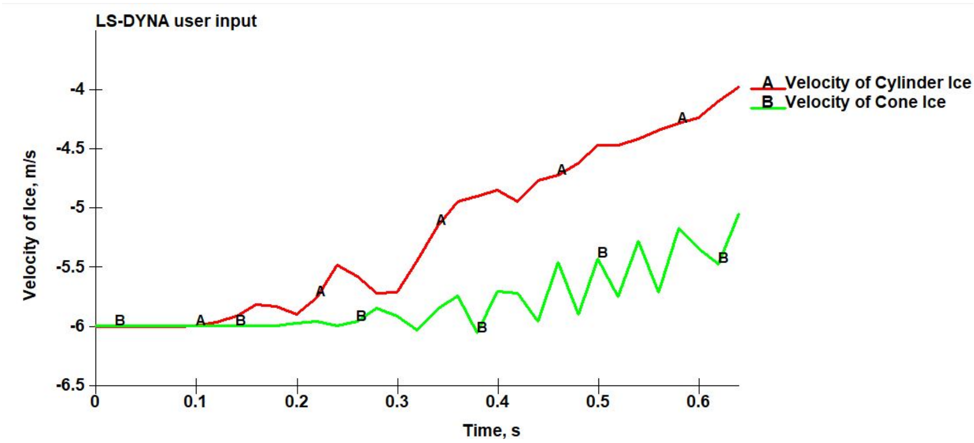

Figure 9.12: Velocity of the Ice during the Impact

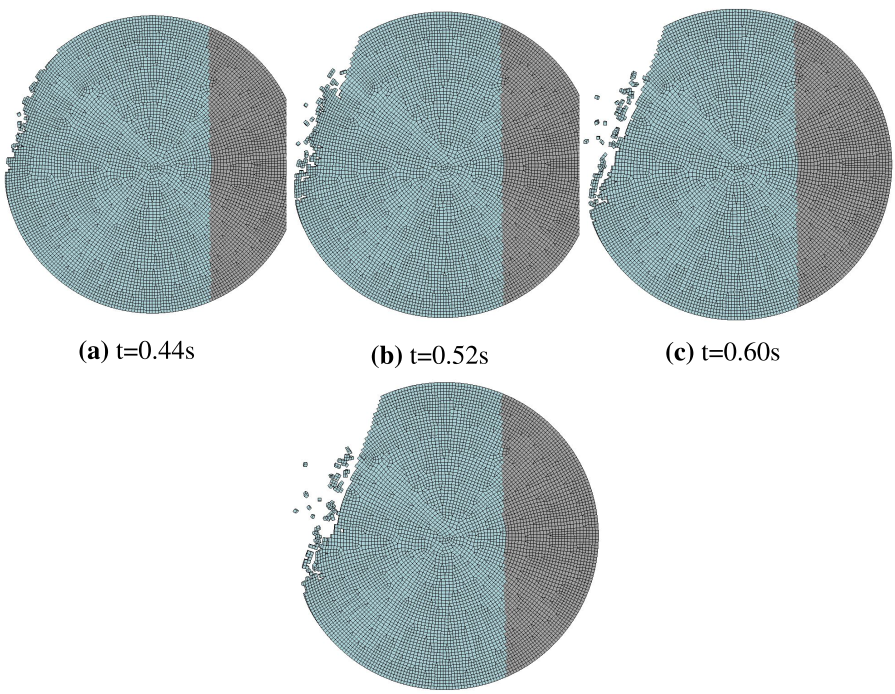

(a) t=0.44s **(b)** t=0.52s **(c)** t=0.60s

(d) t=0.65s

Figure 9.13: Cylinder Ice crashed Layer by Layer

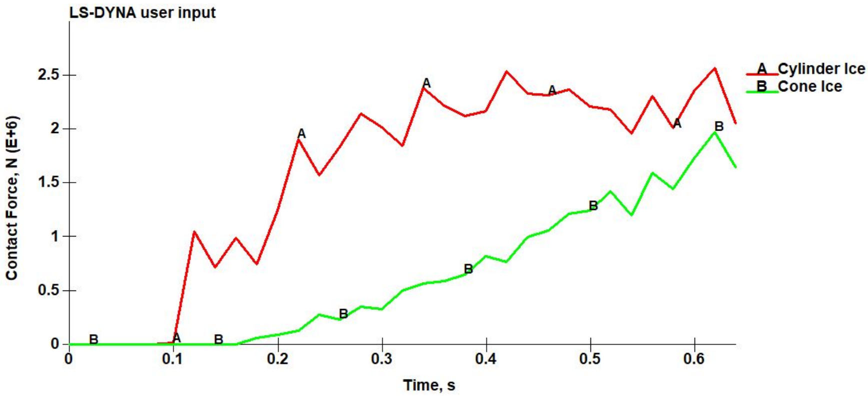

Figure 9.14: Contact Force During the Impact

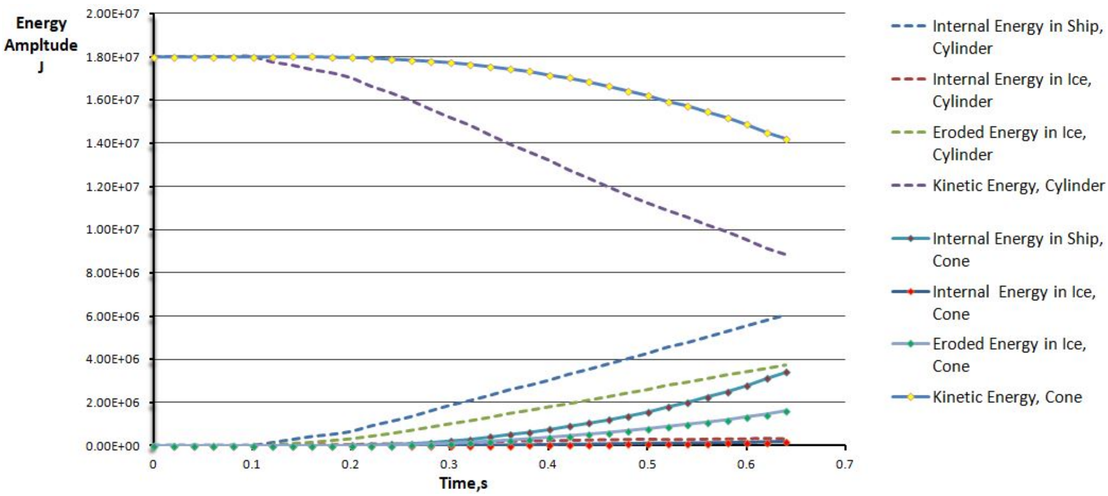

Figure 9.15: Energy Dissipation During the Impact

The energy dissipation during the contact is shown in figure 9.15. There is no eroded energy in ship structures, since fracture doesn't appear on the ship. It shows that there is very little internal energy in the ice, but the eroded energy in the ice is quite big. That means that the ice dissipates the energy mainly by erosion rather than deformation. The internal energy in ship is higher than the eroded energy in ice, which means the ship structures dissipate more energy than the ice, even though the ship structures is relative much more strong than the ice model. There is more internal energy dissipated by ship structures while cylinder ice model is used. That means the cylinder ice model can cause more deformation to the ship structures. Even though the cone ice model has a sharper edge, which appears to have more potential to damage or even penetrate the ship shell locally, but since the ice material is so weak compared to steel, so the sharper ice model will actually be crushed more easily and cause less deformation to the ship structures.

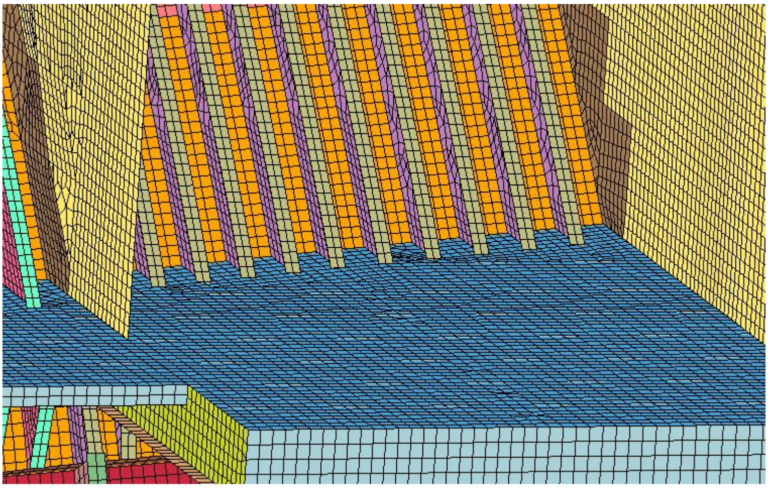

(a) Before Collison

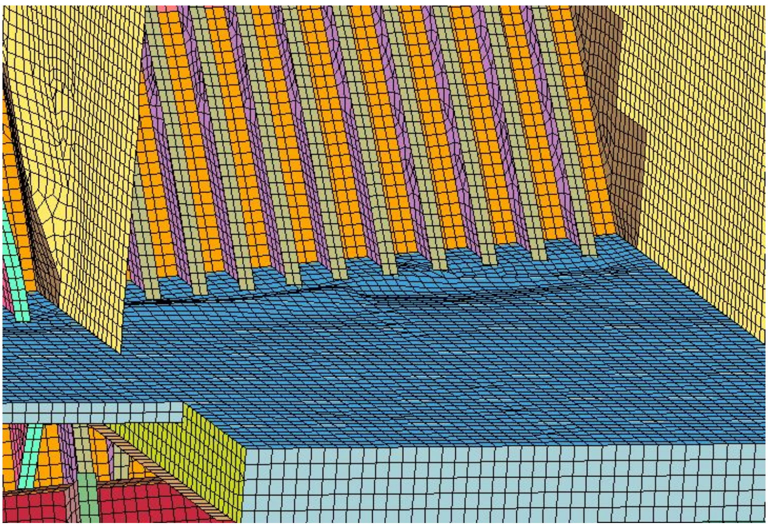

(b) After Collision

Figure 9.16: Buckled Deck and Bulkhead (The blue part is the deck area)

From visual inspection, the ship structure is almost not deformed at all in these two simulations, the reason maybe that the mass of the ice model is too small to involve enough energy to deform the ship. So one more simulation is done, using exactly the same input with the cylinder ice model, except increasing the mass of the ice model to 10000 tons, which can represent the mass of a small berg. From the simulation result, it is found that the ice is still crushed completely, and the ship is not damaged seriously in general. That means the contact reaction is actually restricted by the material strength of ice. The ice is too weak to cause considerable damage to the ship, even with large kinetic energy. But locally, there are some more obvious deformations from visual inspection. For example, the deck below the contact location and the transverse bulkhead is buckled in some extent, as shown in figure 9.16. The collision force will firstly act on the transverse frame, but since the transverse frame is connected to the deck, so the deck will restrict the end of frame from moving. On the contrary, the collision force will be transferred to the deck and leads to buckling. The wider transverse bulkhead is easier to buckle compared to the transverse frame, that is because the bulkhead has a longer buckling length.

9.3 Ship Structures Impact with Multi-year Ice Floe above Ice Strengthen Area

As we can see form the last section, the impact at ice strengthen area with ice floe will not cause any critical damage to the ship structures, because the ship structures there are constructed with enough resistance to crush the ice material. But in reality, the ice floe is also possible to hit the shell above the ice strengthen area due to wave. Beyond the ice strengthen area, the shell plate is thinner and the frame space is wider. So two simulations were run for ship-ice impact above ice strengthen area, to see if the collision will cause some critical damage. Figure 9.17 shows the collision position. High strengthen steel and Mild steel is used for the ship structures separately, to see what happens if the relative strength of steel is reduced. Cone shape ice is used for both simulations.

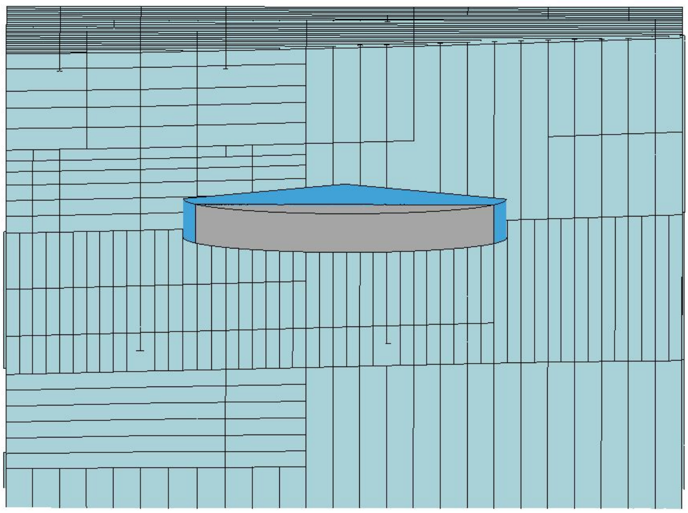

Figure 9.17: Position of Collision above Ice Strenghten Area (Frame arrangement is doubled at the ice Strengthen area. Above the ice strengthen area, the ship structure is framed longitudinally at left, but framed transversely at right)

From visual inspection, the impact with ice floe in this position will cause some more obvious deformation on the ship frames, but no crack appears. Besides, the collision will cause more deformation on the ship shell part, which is framed longitudinally, as shown in figure 9.18.

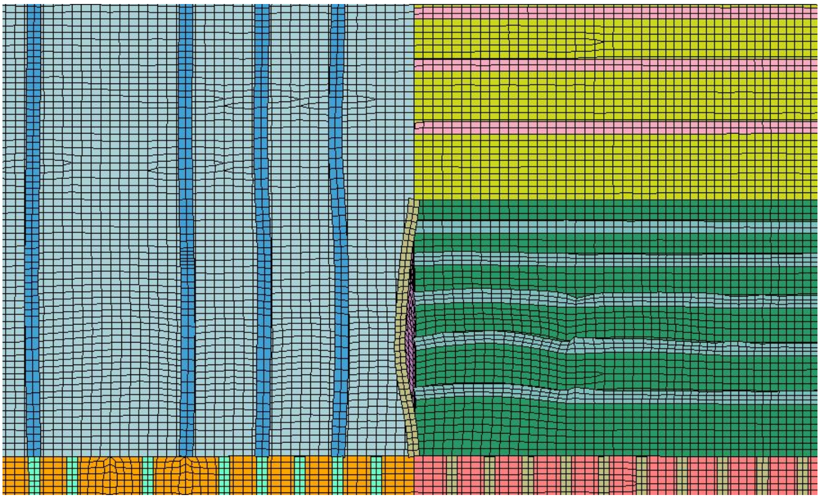

Figure 9.18: Ship Frames Deformation

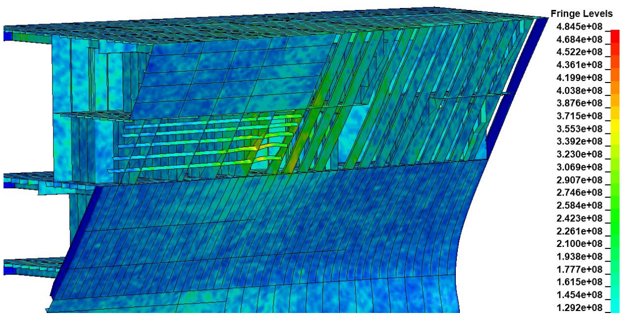

(a) Stress Distribution for High Strength steel

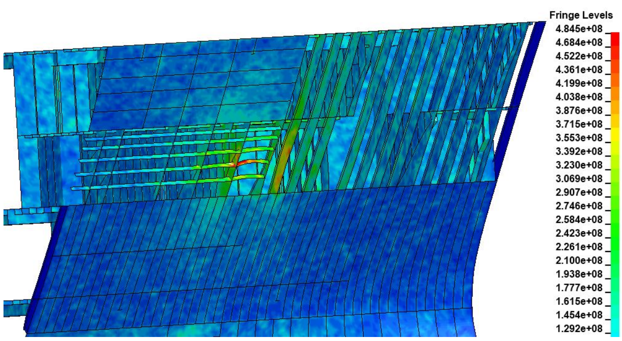

(b) Stress Distribution for Mild steel

Figure 9.19: Stress Distribution at Last Time Step

The longitudinal frames possess less resistance against the ice-floe collision compared to the transverse frame. That is because firstly, the scantlings of longitudinal frames is smaller than transverse frames. Besides, the transverse frame is supported by the deck at the end, but the longitudinal frame is supported by the last transverse frame at then end. See figure 9.18. The deck is a stronger part, which can provide more supporting than the transverse frame. There is lots of out-of plane bending in the last transverse frame. That may because that, after the longitudinal stiffeners are deformed, the end of the longitudinal stiffeners will push the transverse frame to move out of plane.

The stress distribution for ship structure using high strength steel and mild steel is shown in figure 9.19. It shows that the highest stress appears at the longitudinal frame near the contact location. There is more stress developed in the ship structure using mild steel.

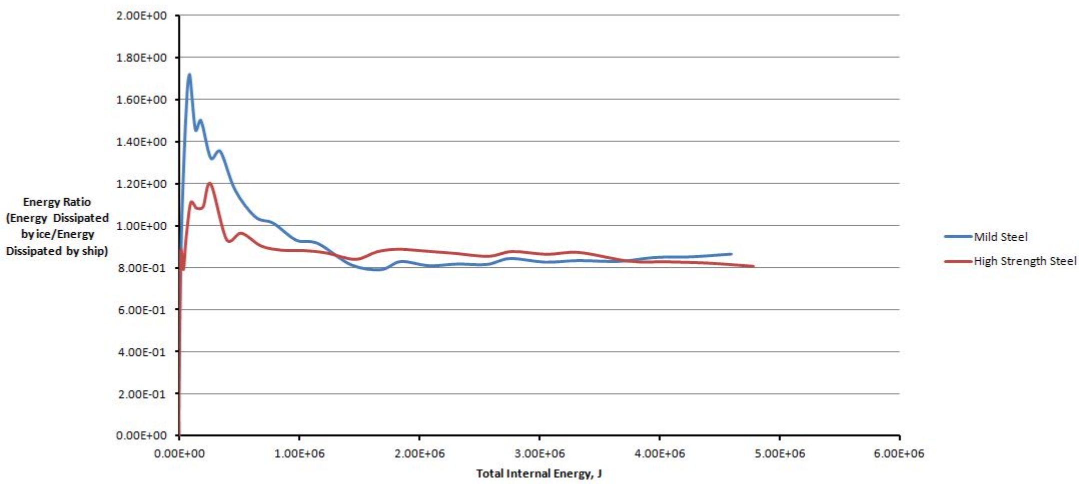

Figure 9.20: Comparison of Energy Dissipation

Figure 9.20 shows the relative energy dissipation in ice and ship structures for both mild steel and high strength steel. The x-axis represents the total dissipated energy by ice and ship structures. The y-axis is energy dissipated by ice normalized by energy dissipated by ship. The energy dissipated by ice includes the strain energy and eroding energy in ice. It shows that, at the beginning, the ice dissipates more energy than ship. That is because the ice has a sharp edge, so it is crushed easily at first and hardly make any deformation on the ship. But during the collision, the ice edge becomes more blunt, and there are more contact areas, so the ship structures were deformed finally. That produces lots of strain energy in ship, so the energy dissipated by ice becomes less compared to the energy dissipated by ship. Besides, it also shows that at the beginning, the ice model tends to dissipate more energy while mild steel is using, compared to high strength steel. The reason for this is that the Young's Modulus for Mild steel is higher than the High strength steel (as shown in table 8.2, 8.3). So at the beginning, within the elastic range, the Mild steel is actually stiffer than the High strength steel. So the ice model tends to dissipate more energy while contacting with mild steel ship structures, because the ice is more weaker compared to ship structures.

The collision above ice strengthen area will cause more deformation to the ship structures, and leave some plastic deformation. But no part is critical to have cracks, so the overall integrity will not be impaired.

9.4 Ship Structures Impact with uncrushable Cone Ice Floe

As we can see from the result in the last two sections, the Multi-year ice floe can cause only slight deformation on the ship structures. The ship is designed with enough resistance against collision with ice floe and the ice is completely crushed by the ship. During the thesis work, several simulations are run with an error in it, which is mentioned in chapter 8.3.4. That mistake makes the ice uncrushable. Even though that simulation is not realistic but it is interesting to present what happens if the ice is not crushed. Cone shape ice model is used. The similar boundary conditions are used to prevent the ice from slipping down, as shown in figure 9.11. The total mass of the ice including the rigid part is also 1000t and the initial velocity is 6m/s.

Several different contact locations are selected for this ice model. The first location is at the ice strengthen area, and on top of the transverse frame. The second location is also at the ice strengthen area, but in between the frames. Then, since the transverse frame is arranged for half frame space at ice strengthen area, but only arranged for one frame space at other area, so the third contact location is selected above the ice strengthen area and in between two frames. Figure 9.21 shows the frame space compared to the size of the ice model for location 2 and location 3. From the figures we can see that the shape of the ice is quite 'blunt' compared to the frame space. In other word, the aspect ration of the shape of ice, which is defined in chapter 5.1.3, is quite small. This makes it difficult to penetrate the ship side shell. One suggestion here is that, it is possible to increase the potential of penetrating the shell by decreasing the angle indicated in figure 9.21.

The several items, which can be used to justify the quality of the numerical simulation results are listed in Appendix II and III. The important results of the three different locations are compared and discussed below.

The ship side shell is not penetrated by the ice model in all three contact locations but the impact caused considerable deformation on ship side shell, which is shown in figure 9.22. The ice model is deformed so that the edge becomes too blunt to penetrate the ship shell.

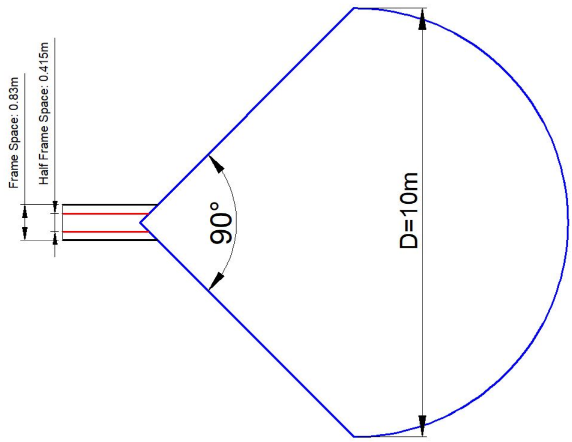

Figure 9.21: Frame Space compared to Ice Size

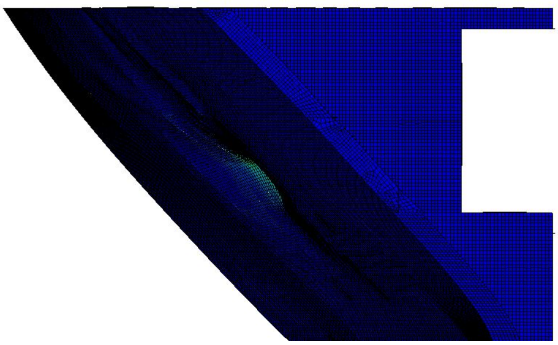

(a) Ship Side Shell Deformation, green area has plastic strain

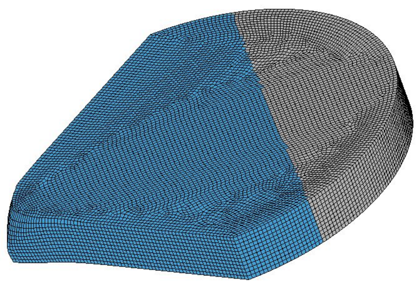

(b) Ice Model Deformation

Figure 9.22: Illustration of Deformation

The stress distribution of the ship structure during maximum deformation is shown in Figure 9.23, for 3 different Locations. Figure 9.23 (a) shows that there is some initial stress in the ship structure, before the ship structure is contacted with the ice model. However, there is no other load added on the ship structure except the impact load from the ice. This initial stress may caused by the inaccuracy of modeling mentioned in chapter 8.1.1, and illustrated by figure 8.5. This modeling inaccuracy may cause some initial penetration, which will lead some stress in the element. The most natural way to deal with this problem is definitely by refining the model. But that involves very cumbersome work. However the maximum amplitude of the initial stress is only around 2MP, which is far lower than the stress from impact, so it is considered that this initial stress will not affect the stress distribution during impact significantly.

The stress distribution for largest deformation for 3 locations shows that there is quite high stress concentration area at the contact location. The area which is far away from the contact location is only affected by the impact slightly. One interesting thing is that the stress tends to develop toward the longitudinal framed shell, which is shown in all 3 cases, at the left downward corner of the shell. This indicates that the transversely stiffened shell is more stiff than longitudinally stiffened shell, while subjects to contact load. At some areas far away from collision, there are some sharp triangular elements having abnormal high stress. This problem can be solved by refining the mesh, to avoid sharp elements.

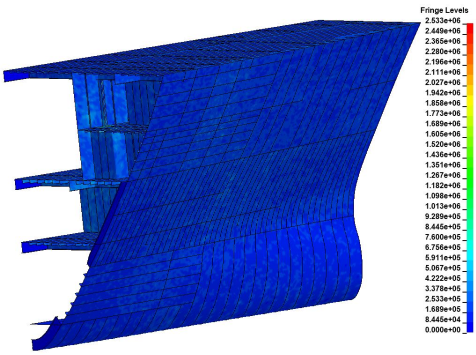

(a) Initial Stress Distribution before Collision

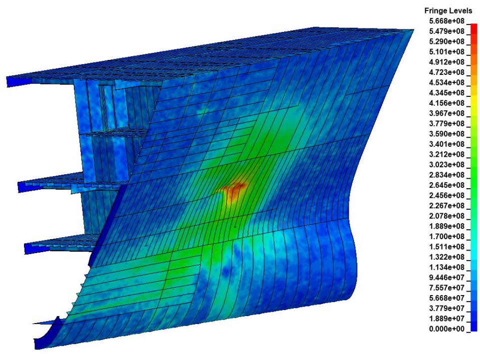

(b) Stress Distribution, Location 1

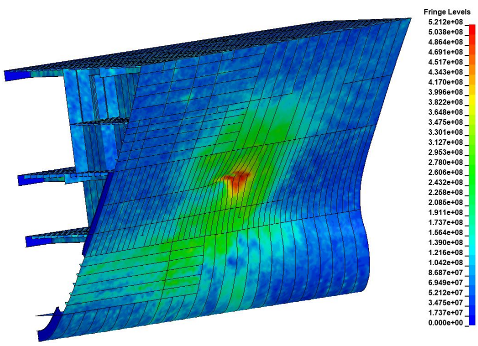

(c) Stress Distribution, Location 2

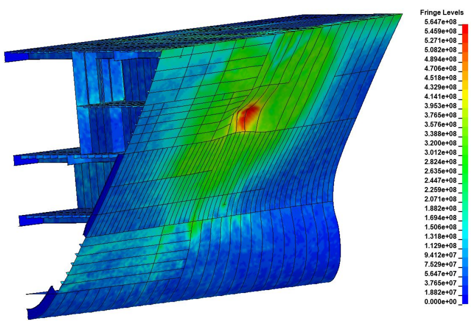

(d) Stress Distribution, Location 3

Figure 9.23: Stress Distribution on Ship Shell while Largest Deformation

The velocity of the ice with respect to time is shown in figure 9.24. The ice at location 3 is stopped earlier than the ice in Location 1 and 2. That is because the initial space between ice and ship shell is set closer than the other two. The ice is near to be stopped at Location 1 and Location 2. At Location 3, the ice is bounced back. While the ice is bounced back, the deformed ship structure is also recovered in some extend, since there are some elastic deformation. The different results between Location 1,2 and Location 3 indicate that the ship structures at Location 3 is more tough than Location 1 and 2. But this is conflicted with the fact that Location 1 and 2 is ice strengthen area but location 3 is not strengthened. The reason is that at location 1 and 2, the ice begins to rotate in its plane and move in y direction as shown in figure 9.27. Because the ship cross section is shallower toward the bow, some velocity in X-direction stays.

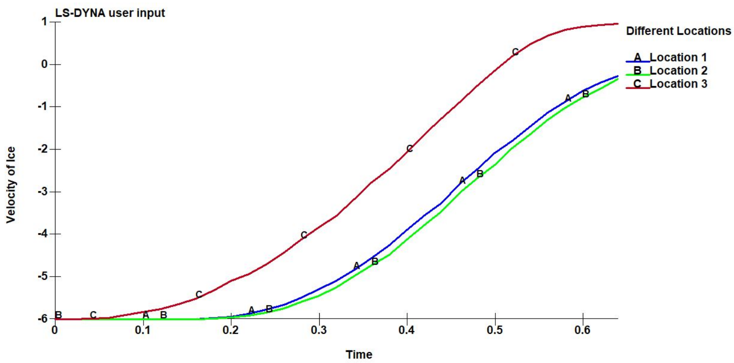

Figure 9.24: Velocity of the ICE in X-direction, Unit: Velocity m/s; Time s

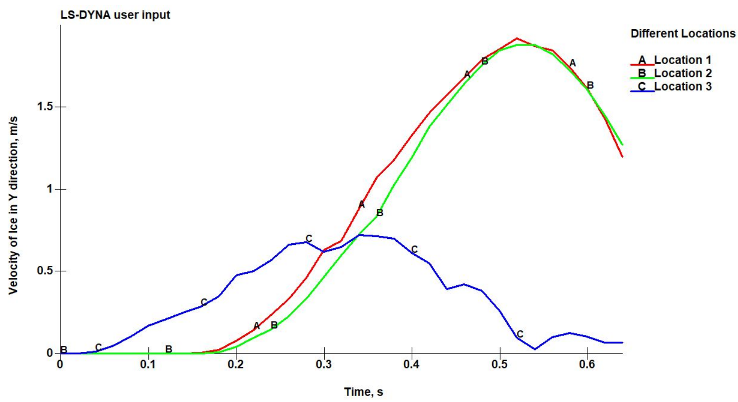

Figure 9.25: Velocity of Ice in Y-direction

Figure 9.26 shows the development of strain energy in ship structures and ice. The solid line represents the total strain energy in both ship and ice, but the shaded line represents the strain energy only in ice. It shows that the ice dissipates near to one third of the total strain energy. The ice is quite strong compared to the ship structures. There are more strain energy developed in Location 3 than Location 1 and 2. This is consistent with the finding in velocity variation. The ice in Location 3 is stopped more so more kinetic energy is dissipated by internal energy.

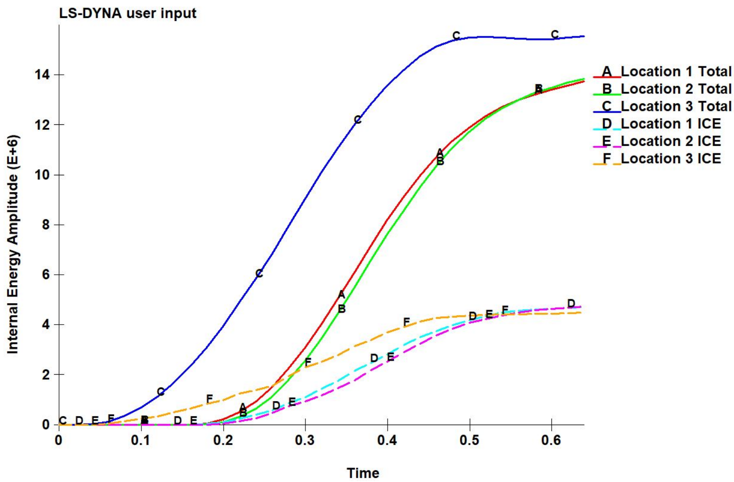

Figure 9.26: Internal Energy in 3 Locations. Total: The total internal energy. Ice: The internal energy in Ice. Unit: Energy J

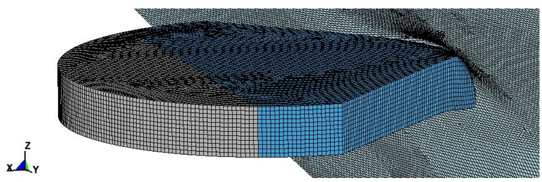

Figure 9.27: Illustration of the Movement of the Ice

Figure 9.28 shows the contact force at 3 locations with respect to time. Compared to figure 9.24, it shows that the contact force begins to drop before the ice is stopped. This may because that the ice begins to move in positive y direction and rotates with respect to z axis.See figure 9.27. This may make the contact between ice and ship side shell less, because the ship has shallower transverse section toward the bow. The contact force at Location 3 is higher than Location 1 and 2. The reason is that frame space is wider at Location 3, See Figure 9.21, so that the ice edge will be embed more in between the frames, so that it will be restricted more from moving in y direction and rotating. Figure 9.25 shows the velocity of ice in Y-direction for 3 locations. It clearly shows that the velocity of Ice at Location 3 in Y-direction is lower than others.

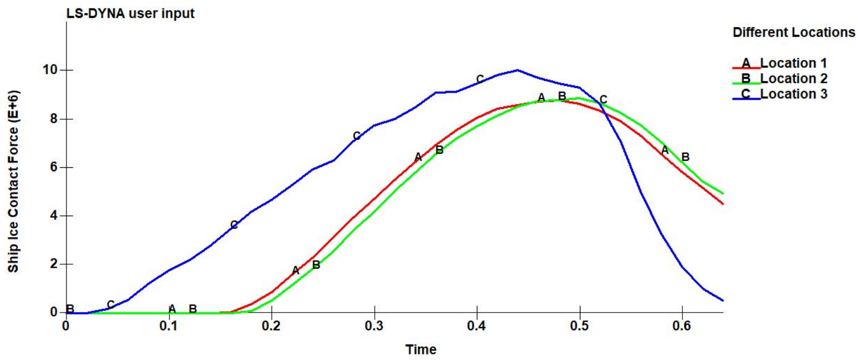

Figure 9.28: Ship-ICE Contact Force in 3 Locations, Unit: Force N

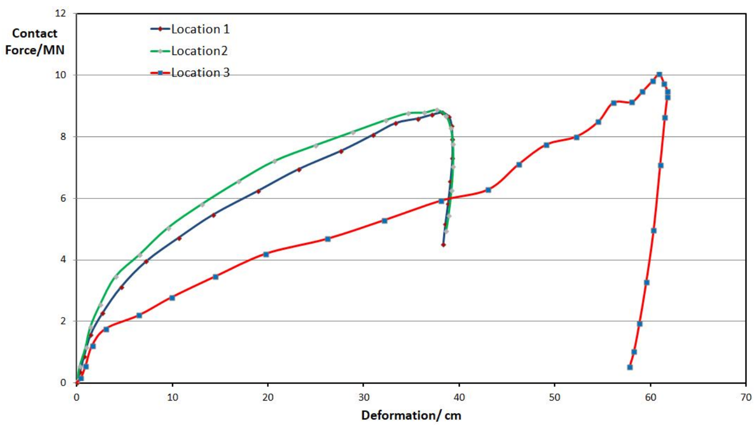

Figure 9.29: Deformation- Contact Force Relationship

The point on ship shell with most deformation is found, and the displacement of that point is plotted with respect to contact force between ship and ice. See Figure 9.29. It shows that firstly there is some elastic deformation, and then huge plastic deformation developed. And after the ice is moving out of this area, the shell begin to recover in some extent, but following the elastic slope. So at the end, there will be some irreversible plastic deformation on the ship shell. Besides, it shows that at the beginning, the stiffness at Location 3 is lower than the stiffness at Location 1 and 2. This is consistent with the fact that the frame spacing at location 3 is twice the frame spacing at location 1 and 2, and the shell plate is thinner. But the contact force gets higher level at Location 3, because the ice is embed more in between the frames.

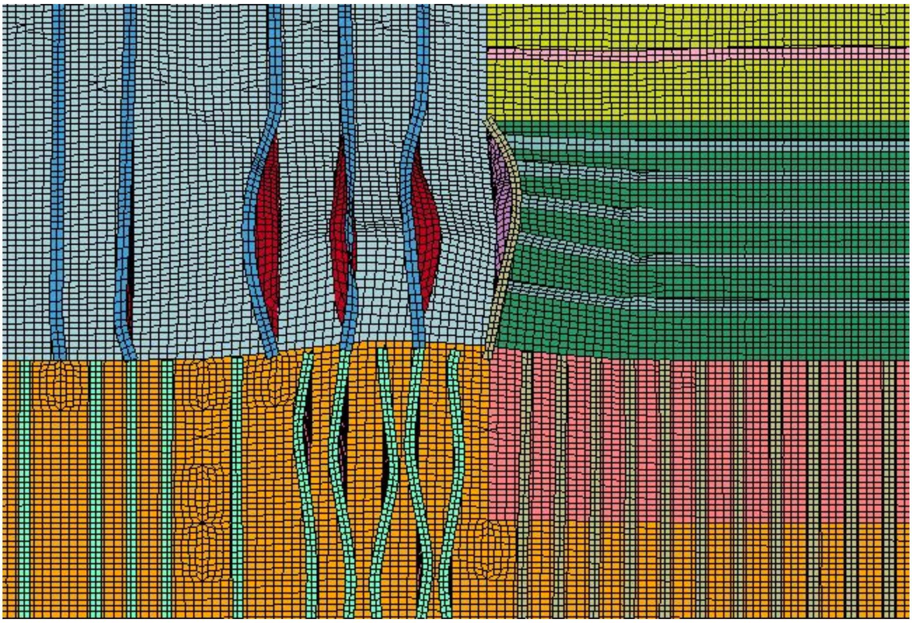

Figure 9.30: Deformation of Frames and Side Shell

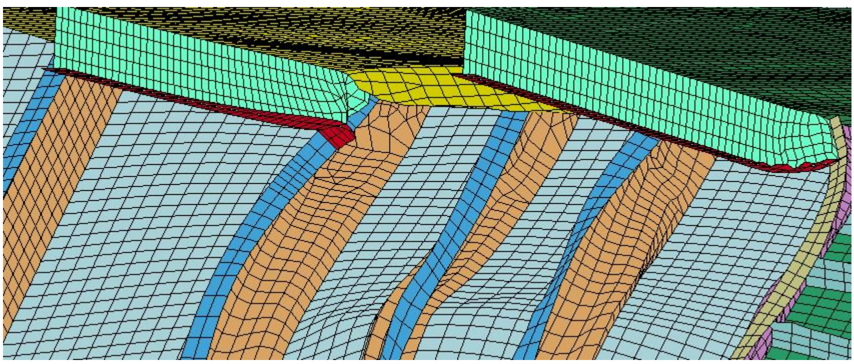

Figure 9.31: Deformation of Transverse Girder and Deck

Figure 9.30 and figure 9.31 shows the deformation of ship structures, when the ice floe hits above ice strengthen area. As we can see, the uncrushable ice will cause more serious damage to the ship structures. The transversely framed shell doesn't have enough strength to resist the collision. Comparing to figure 9.18, the only difference in these two simulations are the ice material model, but the frame was deformed much more seriously this time. When the ice floe is crushed, the transverse frame has enough resistance against the collision, only the longitudinal frame is deformed. But when the ice is not crushed, the transverse frame is bent out of plane. The contact location is above ice strengthen area, but the frame at the ice strengthen area, which is denser, is also deformed. Figure 9.31 shows that the transverse girder is buckled along with deck. Since the end of the girder is connected to the transverse frame, the contact force is transferred to the girder as an axial force.

Chapter 10

Conclusions and Recommendations for Further Work

From the simulations, we can see that the ship is designed with enough resistance against ice-floe impact. The ice-floe cannot penetrate the ship shell and is completely crushed by the ship. There is only slight plastic deformation in the ship structures. The collision happened beyond ice strengthen area can cause more deformation. The impact force is restricted by the material strength of ice. If the ice material is set uncrushable, then the ice-floe will cause much more deformation on the ship structures. A rigid body can tear up the ship shell easily. The reason is that the rigid body cannot deform,, so the sharp edge will cause huge stress concentration at the impact point, and then cracks appear there.

Based on the work in this thesis and on the given conclusions some recommendations for further work can be given.

Find the reason and eliminate the initial stress in the ship model. The most natural way is to eliminate all the initial penetrations in the ship model, but that will involve too much modeling work.

Find the reason for the negative sliding energy. The sliding energy is caused by the erosion of solid elements. And the geometry of the ice model may have some connection with it, since negative sliding energy only appears when cone shaped ice is used, but not for cylinder shaped ice.

Find the most critical impact scenario, that may cause penetration on the ship shell. From this master thesis work, it is found that ice model with a sharper edge maybe more difficult to penetrate the ship shell, since it is easier to be crushed.

Find a method to simulate the interaction with water more correctly. The water can provide buoyancy force, drag force and added mass force to support the ice floe.

The external mechanism is not considered in this master thesis work. The ship structure is basically fixed to impact with ice floe. It maybe appropriate if the ship structure is large enough, and the ship will simply crush the ice. However, if the ice model is strong enough to excite motion or cause deformation to ship structures, it is better to take external mechanism into consideration.

Bibliography

[1] Hagbart S Alsos, Jørgen Amdahl, and Odd S Hopperstad. On the resistance to penetration of stiffened plates, part ii: Numerical analysis. *International Journal of Impact Engineering*, 36(7):875–887, 2009.

[2] Trevor Butler. Iacs polar class requirements and hull structural design applications. *Marine Technology and SNAME News*, 46(2):16–17, 2009.

[3] CG Daley. Energy based ice collision forces. In *Proceedings of the 15th International Conference on Port and Ocean Engineering under Arctic Conditions, Helsinki University of Technology in Espoo, Finland*, 1999.

[4] Claude Daley. Background notes to design ice loads. *IACS Ad-hoc Group on Polar Class Ships and Transport Canada*, 2000.

[5] John O Hallquist et al. Ls-dyna theory manual. *Livermore software Technology corporation*, 3:25–31, 2006.

[6] B Hill. Ship collision with iceberg database. 2006.

[7] Zhenhui Liu. Analytical and numerical analysis of iceberg collisions with ship structures, 2011.

[8] Zhenhui Liu, Jørgen Amdahl, and Sveinung Løset. Integrated numerical analysis of an iceberg collision with a foreship structure. *Marine Structures*, 24(4):377–395, 2011.

[9] Zhenhui Liu and Jørgen Amdahl. A new formulation of the impact mechanics of ship collisions and its application to a ship–iceberg collision. *Marine Structures*, 23(3):360–384, 2010.

[10] Zhenhui Liu, Jørgen Amdahl, and Sveinung Løset. Plasticity based material modelling of ice and its application to ship–iceberg impacts. *Cold Regions Science and Technology*, 65(3):326–334, 2011.

[11] Sveinung Løset. Thermal energy conservation in icebergs and tracking by temperature. *Journal of Geophysical Research: Oceans*, 98(C6):10001–10012, 1993.

[12] LS-DYNA Keyword User's Manual. Version 971. *Livermore Software Technology Corporation*, 7374, 2007.

[13] P Terndrup Pedersen and Shengming Zhang. On impact mechanics in ship collisions. *Marine Structures*, 11(10):429–449, 1998.

[14] Kaj Riska. Design of ice breaking ships. 2011.

[15] Martin Storheim, teknikk Norges teknisk-naturvitenskapelige universitet Institutt for marin, and universitet Norges teknisk naturvitenskapelige. *Structural response in ship-platform and ship-ice collisions*. Thesis, 2016. Avhandling (ph.d.) – Norges teknisk-naturvitenskapelige universitet, Trondheim, 2016.

[16] William James Stronge. *Impact mechanics*. Cambridge university press, 2004.

[17] LS-DYNA Version. 970'. *Livermore Software Technologies Corporation, LSTC Technical Support*, 2006.

Appendix

Appendix I: Input file in Ls-Dyna

```
$# LS-DYNA Keyword file created by LS-PrePost 4.1 - 09Aug2015(14:00)
$# Created on May-30-2017 (11:46:39)
*KEYWORD MEMORY=30000000
*TITLE
$#                                                                         title

*CONTROL_BULK_VISCOSITY
$#        q1        q2      type     btype
  1.500000 6.0000E-2         1         0
*CONTROL_CONTACT
$#  slsfac    rwpnal    islchk    shlthk    penopt    thkchg     orien    enmass
  0.100000     0.000         2         0         1         1         1         0
$#  usrstr    usrfrc     nsbcs    interm     xpene     ssthk      ecdt   tiedprj
         0         0        10         0  4.000000         0         0         0
$#   sfric     dfric       edc       vfc        th     th_sf    pen_sf
     0.000     0.000     0.000     0.000     0.000     0.000     0.000
$#  ignore    frceng   skiprwg    outseg   spotstp   spotdel   spothin
         0         0         0         0         0         0     0.000
$#    isym    nserod    rwgaps    rwgdth     rwksf      icov    swradf    ithoff
         0         0         1     0.000  1.000000         0     0.000         0
$#  shledg    pstiff    ithcnt    tdcnof     ftall    unused    shltrw
         0         0         0         0         0               0.000
*CONTROL_COUPLING
$#  unleng    untime    unforc    timidl     flipx     flipy     flipz    subcyl
  1.000000  1.000000  1.000000     0.000         0         0         0         1
*CONTROL_CPU
$#  cputim
     0.000
*CONTROL_DYNAMIC_RELAXATION
$#  nrcyck     drtol    drfctr    drterm    tssfdr    irelal     edttl    idrflg
       250 1.0000E-3  0.9950001.0000E+30  0.900000         0 4.0000E-2         0
*CONTROL_ENERGY
$#    hgen      rwen    slnten     rylen
         2         2         2         1
*CONTROL_HOURGLASS
$#     ihq        qh
         1  0.100000
```

Figure 10.1: Controlling Options A

```
*CONTROL_OUTPUT
$#   npopt    neecho    nrefup    iaccop     opifs    ipnint    ikedit    iflush
         0         3         0         0     0.000         0         0      5000
$#   iprtf    ierode     tet10    msgmax    ipcurv      gmdt   ipldblt      eocs
         0         0         2        50         0     0.000         0         0
*CONTROL_SHELL
$#  wrpang     esort     irnxx    istupd    theory       bwc     miter      proj
 20.000000         2        -1         0         2         2         1         0
$# rotascl    intgrd    lamsht    cstyp6    tshell
  1.000000         0         0         1         0
$# psstupd    sidt4tu    cntco    itsflg    irquad
         0         0         0         0         2
$#  nfail1    nfail4   psnfail    keepcs     delfr   drcpsid    drcprm
         0         0         0         0         0         0  1.000000
*CONTROL_TERMINATION
$#  endtim    endcyc     dtmin    endeng    endmas
  0.650000         0     0.000     0.000     0.000
*CONTROL_TIMESTEP
$#  dtinit    tssfac      isdo    tslimt     dt2ms      lctm     erode     mslst
     0.000  0.900000         0     0.000     0.000         0         0         0
$#  dt2msf   dt2mslc     imscl    unused    unused     rmscl
     0.000         0         0                         0.000
```

Figure 10.2: Controlling Options B

```
*CONTACT_AUTOMATIC_SINGLE_SURFACE_ID
$#     cid                                                                 title
         2shipself
$#    ssid      msid     sstyp     mstyp    sboxid    mboxid       spr       mpr
         0         1         0         2         0         0         1         1
$#      fs        fd        dc        vc       vdc    penchk        bt        dt
  0.300000  0.200000     0.000     0.000     0.000         0     0.0001.0000E+20
$#     sfs       sfm       sst       mst      sfst      sfmt       fsf       vsf
  1.000000  1.000000     0.000     0.000  1.000000  1.000000  1.000000  1.000000
$#    soft    sofscl    lcidab    maxpar     sbopt     depth     bsort    frcfrq
         0  0.100000         0  1.025000  2.000000         2         0         1
$#  penmax    thkopt    shlthk     snlog      isym     i2d3d    sldthk    sldstf
     0.000         0         0         0         0         0     0.000     0.000
$#    igap    ignodprfac/mpadtstif/mpar2    unused    unused    flangl   cid_rcf
         1         1     0.000     0.000                         0.000         0
$#   q2tri    dtpchk     sfnbr    fnlscl    dnlscl      tcso    tiedid    shledg
         0     0.000     0.000     0.000     0.000         0         0         0
```

Figure 10.3: Contact Definitions A

```
*CONTACT_ERODING_SINGLE_SURFACE_ID
$#     cid                                                                 title
         3ice self
$#    ssid      msid     sstyp     mstyp    sboxid    mboxid       spr       mpr
         0        61         0         3         0         0         1         1
$#      fs        fd        dc        vc       vdc    penchk        bt        dt
  0.150000 5.0000E-2     0.000     0.000     0.000         0     0.0001.0000E+20
$#     sfs       sfm       sst       mst      sfst      sfmt       fsf       vsf
  1.000000  1.000000     0.000     0.000  1.000000  1.000000  1.000000  1.000000
$#    isym    erosop      iadj
         0         0         0
$#    soft    sofscl    lcidab    maxpar     sbopt     depth     bsort    frcfrq
         2  0.100000         0  1.025000  2.000000         2         0         1
$#  penmax    thkopt    shlthk     snlog      isym     i2d3d    sldthk    sldstf
     0.000         0         0         0         0         0     0.000     0.000
$#    igap    ignodprfac/mpadtstif/mpar2    unused    unused    flangl   cid_rcf
         1         1     0.000     0.000                         0.000         0
$#   q2tri    dtpchk     sfnbr    fnlscl    dnlscl      tcso    tiedid    shledg
         0     0.000     0.000     0.000     0.000         0         0         0
*CONTACT_ERODING_SURFACE_TO_SURFACE_ID
$#     cid                                                                 title
         1contact between  ice and ship
$#    ssid      msid     sstyp     mstyp    sboxid    mboxid       spr       mpr
         1        61         2         3         0         0         1         1
$#      fs        fd        dc        vc       vdc    penchk        bt        dt
  0.150000  0.150000     0.000     0.000     0.000         0     0.0001.0000E+20
$#     sfs       sfm       sst       mst      sfst      sfmt       fsf       vsf
  1.000000  1.000000     0.000     0.000  1.000000  1.000000  1.000000  1.000000
$#    isym    erosop      iadj
         0         1         0
$#    soft    sofscl    lcidab    maxpar     sbopt     depth     bsort    frcfrq
         2  0.100000         0  1.025000  2.000000         2         0         1
$#  penmax    thkopt    shlthk     snlog      isym     i2d3d    sldthk    sldstf
     0.000         1         1         0         0         0     0.000     0.000
$#    igap    ignodprfac/mpadtstif/mpar2    unused    unused    flangl   cid_rcf
         1         1     0.000     0.000                         0.000         0
$#   q2tri    dtpchk     sfnbr    fnlscl    dnlscl      tcso    tiedid    shledg
         0     0.000     0.000     0.000     0.000         0         0         0
```

Figure 10.4: Contact Definitions B

```
*MAT_USER_DEFINED_MATERIAL_MODELS_TITLE
RTCL
$#     mid        ro        mt       lmc       nhv    iortho     ibulk        ig
         1 7850.0000        46        16        35         0         4         3
$#   ivect     ifail    itherm    ihyper      ieos      lmca    unused    unused
         1         1         0         0         0         0
$#      p1        p2        p3        p4        p5        p6        p7        p8
2.0400E+11  0.3000007.8900E+10 8.5000E+8 3.3800E+8 7.2800E+8  0.166600 1.5000E-2
$#      p1        p2        p3        p4        p5        p6        p7        p8
  0.320000  1.000000     0.000     0.000     0.000     0.000     0.000     0.000
```

Figure 10.5: User Defined RTCL Steel Material Model Input

```
*MAT_USER_DEFINED_MATERIAL_MODELS_TITLE
ICE MATERIAL
$#     mid        ro        mt       lmc       nhv    iortho     ibulk        ig
         3 900.00000        41         8        20         0         3         4
$#   ivect     ifail    itherm    ihyper      ieos      lmca    unused    unused
         0         1         0         0         0         8
$#      p1        p2        p3        p4        p5        p6        p7        p8
 9.5000E+9  0.300000 7.9167E+9 3.6538E+92.2930E+13 2.0600E+6 -2.300E-2 -2.000E+6
$#      p1        p2        p3        p4        p5        p6        p7        p8
  1.000000 1.0000E-2     0.000     0.000     0.000     0.000     0.000     0.000
```

Figure 10.6: User Defined Ice Material Model Input

Appendix II: Energy Ratio for all Simulations with Ice Material

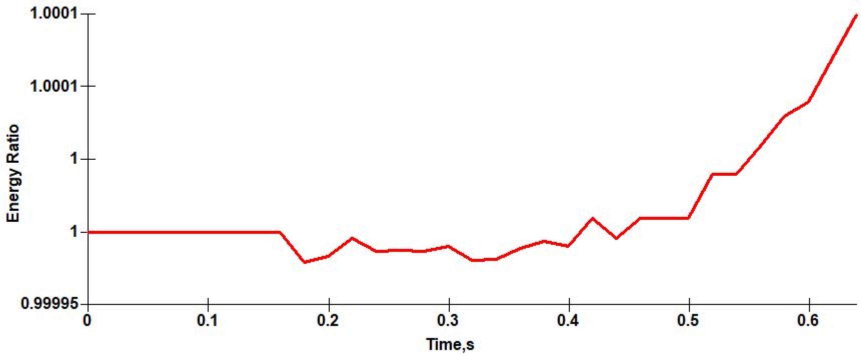

Figure 10.7: Simulation 9.2, Cone Ice

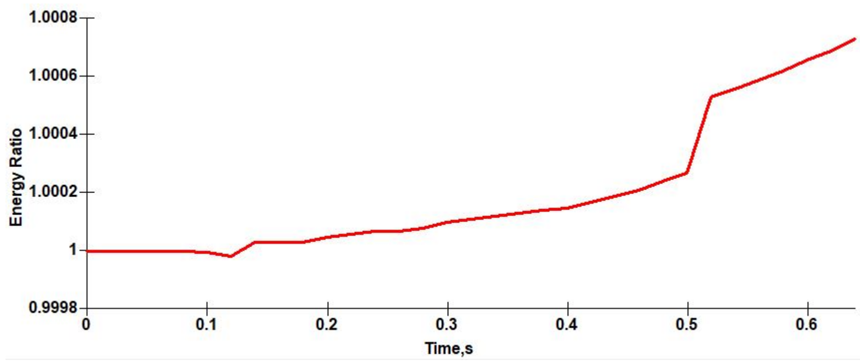

Figure 10.8: Simulation 9.2, Cylinder Ice

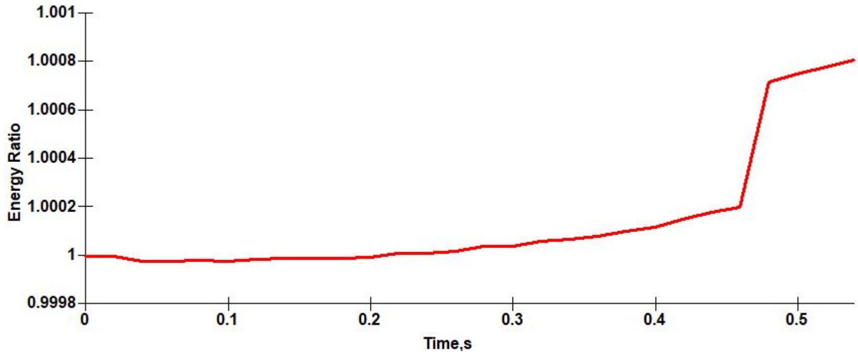

Figure 10.9: Simulation 9.3, High Strength Steel

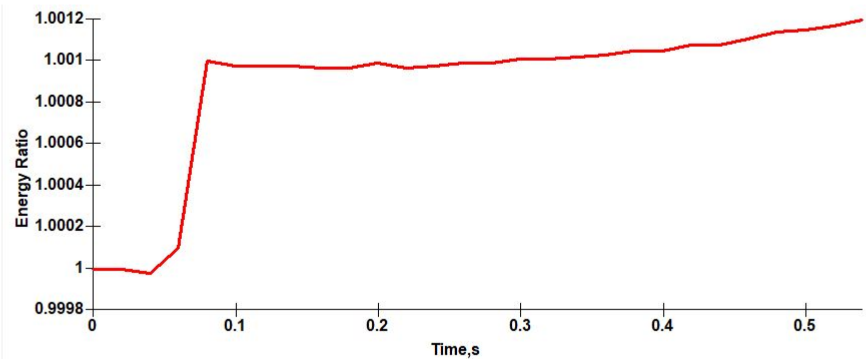

Figure 10.10: Simulation 9.3, Mild Steel

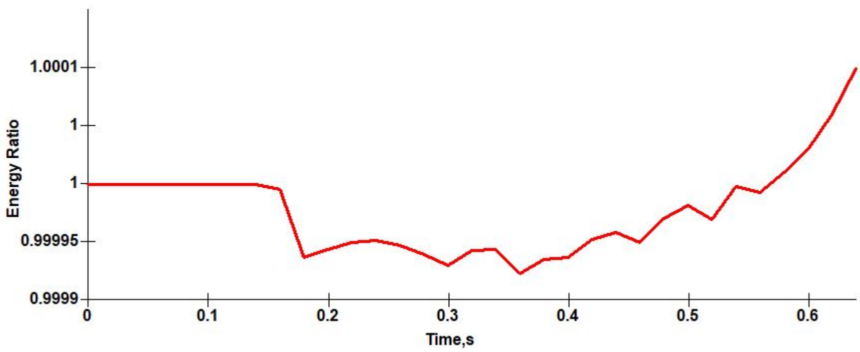

Figure 10.11: Simulation 9.4, Position A

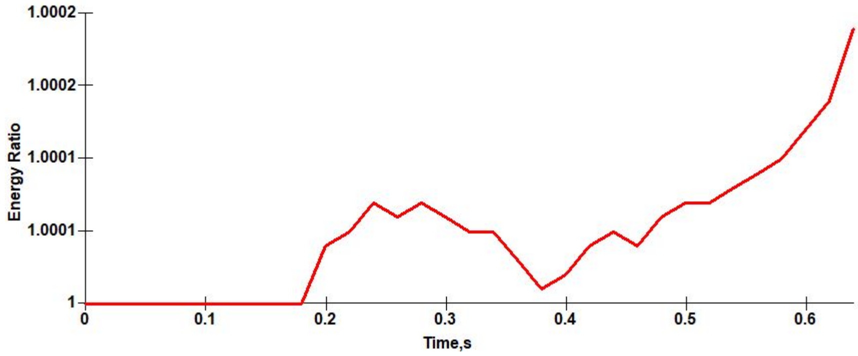

Figure 10.12: Simulation 9.4, Position B

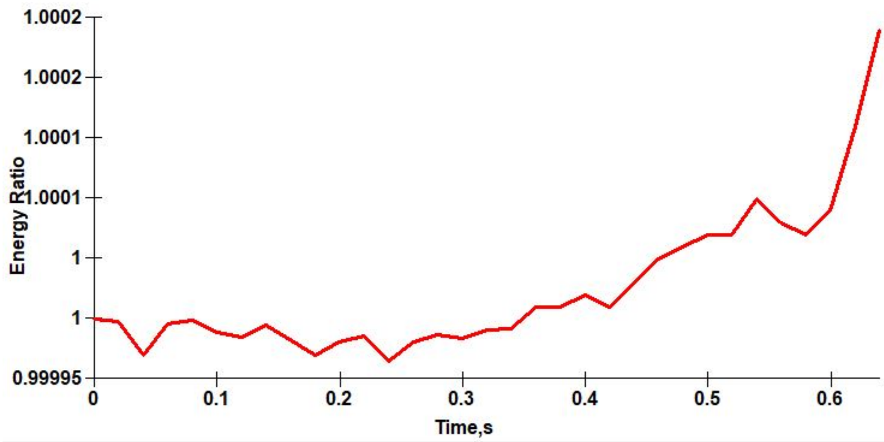

Figure 10.13: Simulation 9.4, Position C

Appendix III: Sliding Energy and Hourglass Energy for all simulations

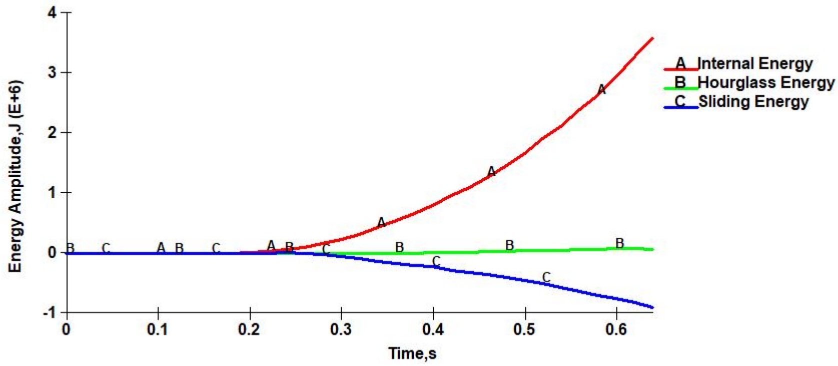

Figure 10.14: Simulation 9.2, Cone Ice

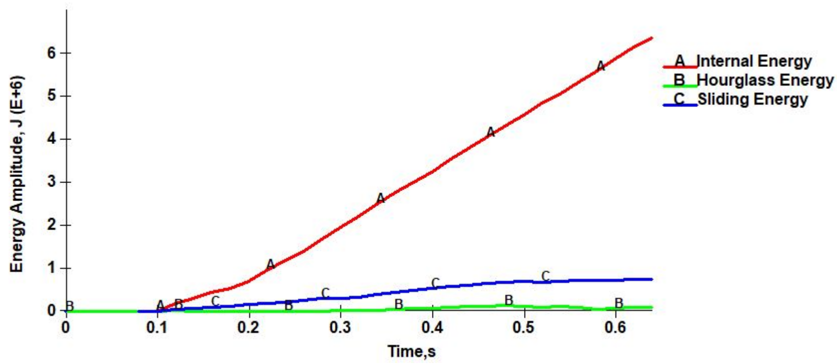

Figure 10.15: Simulation 9.2, Cylinder Ice

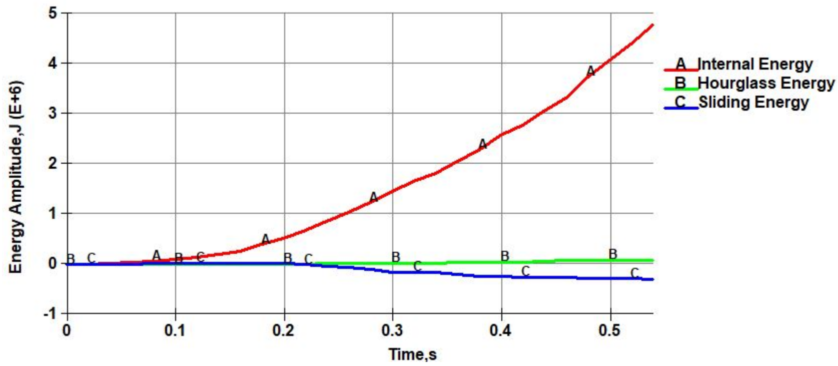

Figure 10.16: Simulation 9.3, High Strength Steel

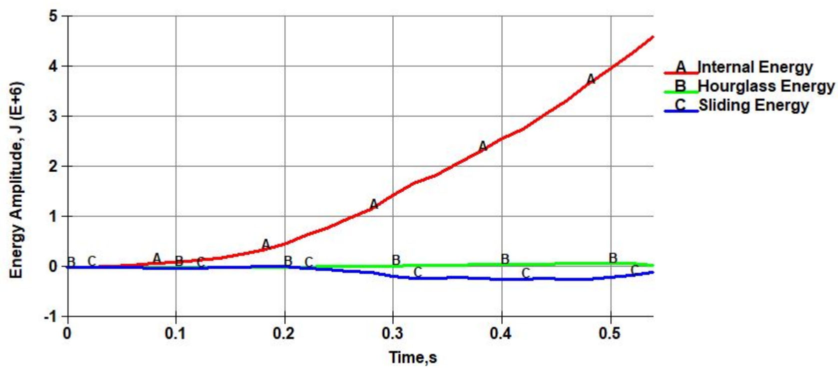

Figure 10.17: Simulation 9.3, Mild Steel

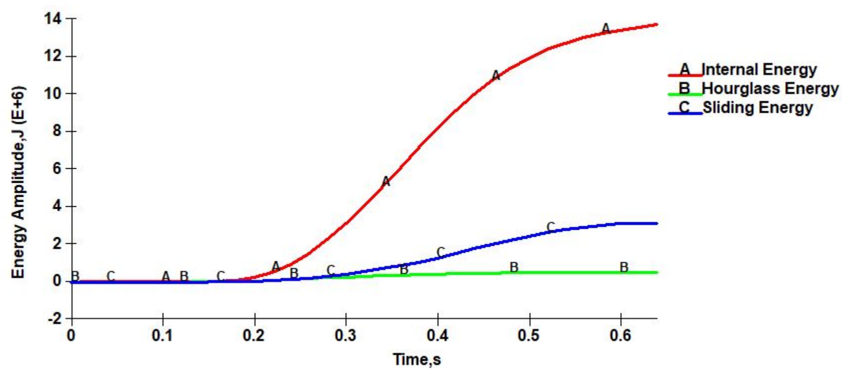

Figure 10.18: Simulation 9.4, Position A

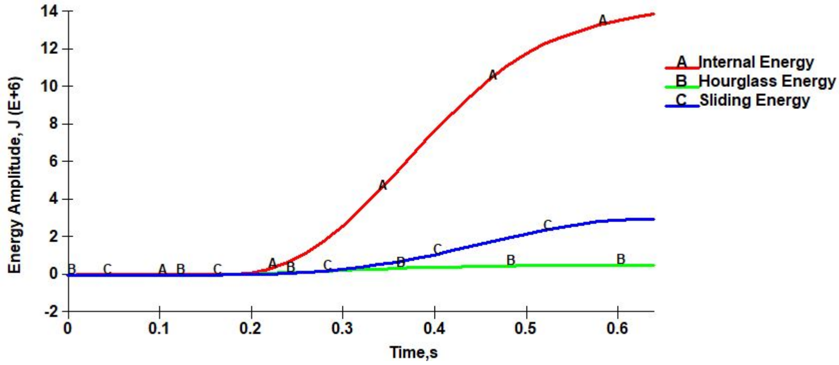

Figure 10.19: Simulation 9.4, Position B

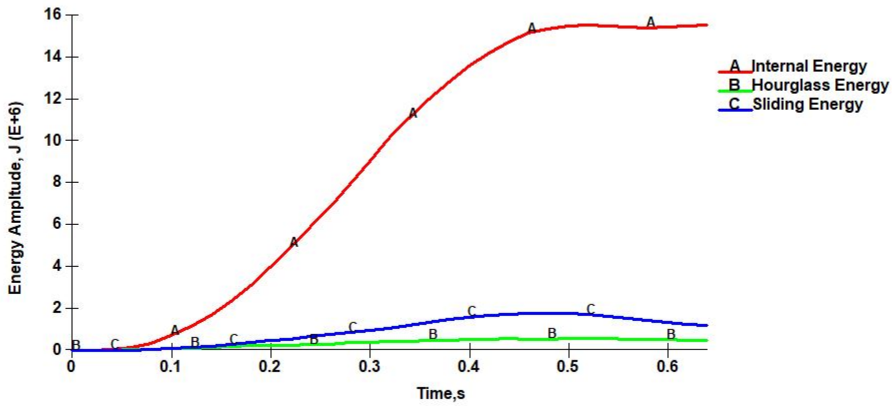

Figure 10.20: Simulation 9.4, Position C